

AD-A038 807

PANAMETRICS INC WALTHAM MASS
ANALYSIS OF GROUND STATION MAGNETOMETER DATA OBTAINED DURING TH--ETC(U)
DEC 76 F A HANSER, B SELLERS

F/G 20/3

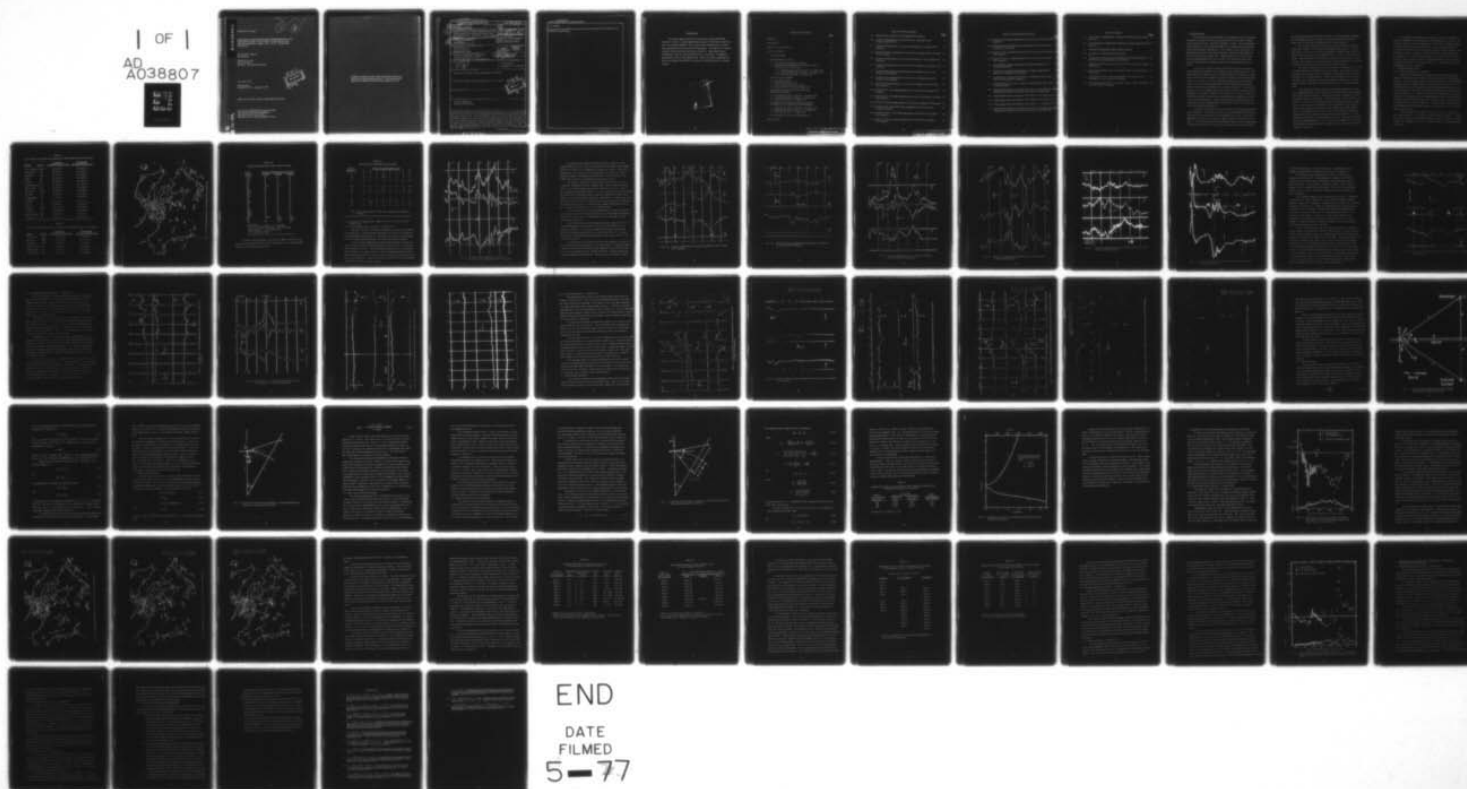
F19628-76-C-0121

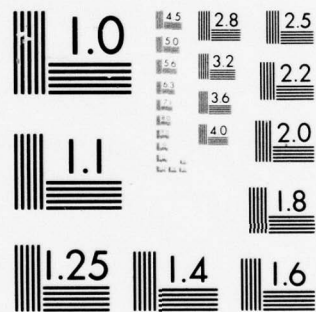
NL

UNCLASSIFIED

AFGL-TR-77-0043

1 OF 1
AD
A038807





MICROCOPY RESOLUTION TEST CHART
NATIONAL BUREAU OF STANDARDS-1963-A

AD A 038807

AFGL-TR-77-0043 ✓

ANALYSIS OF GROUND STATION MAGNETOMETER DATA
OBTAINED DURING THE ROCKET LAUNCHES IN THE
AEOLUS PROGRAM, APRIL 1975, AT FT. CHURCHILL,
MANITOBA

Frederick A. Hanser
Bach Sellers

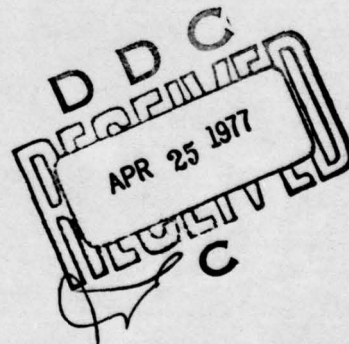
Panametrics, Inc.
221 Crescent St.
Waltham, Massachusetts 02154

December 1976

Final Report
December 1975 - December 1976

Approved for public release; distribution unlimited.

AIR FORCE GEOPHYSICS LABORATORY
AIR FORCE SYSTEMS COMMAND
UNITED STATES AIR FORCE
HANSCOM AFB, MASSACHUSETTS 07131



NO. _____
DC FILE COPY

Qualified requestors may obtain additional copies from the Defense Documentation Center. All others should apply to the National Technical Information Service.

Unclassified

SECURITY CLASSIFICATION OF THIS PAGE (When Data Entered)

19 REPORT DOCUMENTATION PAGE		READ INSTRUCTIONS BEFORE COMPLETING FORM	
18 1. REPORT NUMBER	2. GOVT ACCESSION NO.	3. RECIPIENT'S CATALOG NUMBER	
6 2. TITLE (and Subtitle)	5. TYPE OF REPORT & PERIOD COVERED		
Analysis of Ground Station Magnetometer Data Obtained During the Rocket Launches in the AEOLUS Program, April 1975, at Ft. Churchill, Manitoba	Final Report, Dec 1975 - Dec 1976		
10 3. AUTHOR	6. PERFORMING ORG. REPORT NUMBER		
Frederick A. Hanser Bach Sellers	Final Report		
9. PERFORMING ORGANIZATION NAME AND ADDRESS		8. CONTRACT OR GRANT NUMBER(s)	
Panametrics, Inc. ✓ 221 Crescent St. Waltham MA 02154		15 F19628-76-C-0121	
11. CONTROLLING OFFICE NAME AND ADDRESS		10. PROGRAM ELEMENT, PROJECT, TASK AND AWC UNIT NUMBERS	
Air Force Geophysics Laboratory Hanscom AFB, Mass. 01731 Contract Monitor: A.F. Quesada/LKD		16 62101F 17 14 76351405	
14. MONITORING AGENCY NAME & ADDRESS (if different from Controlling Office)		12. REPORT DATE	
12 72p.		11 December 1976	
		13. NUMBER OF PAGES	
		71	
		15. SECURITY CLASS. (of this report)	
		Unclassified	
		15a. DECLASSIFICATION DOWNGRADING SCHEDULE	
16. DISTRIBUTION STATEMENT (of this Report)			
Approved for public release; distribution unlimited.			
17. DISTRIBUTION STATEMENT (of the abstract entered in Block 20, if different from Report)			
18. SUPPLEMENTARY NOTES			
19. KEY WORDS (Continue on reverse side if necessary and identify by block number)			
Auroral Electrojet Magnetic Disturbance			
20. ABSTRACT (Continue on reverse side if necessary and identify by block number)			
Magnetometer data from more than a dozen ground stations near the Ft. Churchill part of the Auroral Zone have been obtained and analyzed for the AEOLUS rocket launches in April 1975. The magnetically active launch of 10 April showed con- siderable activity starting to the west of, and moving into, the Ft. Churchill area. The quiet launch of 21 April showed little activity. The auroral launch of 25 April was accompanied by magnetic activity, though not as intense as that of 10 April. Electrojet calculations show that conditions on 10 April were very			

DDC
RECEIVED
APR 25 1977
C

Unclassified

SECURITY CLASSIFICATION OF THIS PAGE (When Data Entered)

403420

Unclassified

SECURITY CLASSIFICATION OF THIS PAGE(When Data Entered)

20. (cont'd)

→ promising for high altitude wave generation that might be observable in the chemical release data. ↗

Unclassified

SECURITY CLASSIFICATION OF THIS PAGE(When Data Entered)

FOREWORD

The work reported herein was carried out under Contract No. F19628-76-C-0121. Special appreciation is given to Malcolm A. MacLeod LKC, the Contract Monitor, whose interest and comments have contributed significantly to the success of this program. The help of Dr. Gordon Rostoker of the University of Alberta, and of Dr. John Walker of the Department of Energy, Mines and Resources, of Canada, in supplying magnetometer data is also appreciated. Most of the other magnetometer data were obtained from WDC-A for Solar-Terrestrial Physics (Geomagnetism).

ACCESSION No.	
NTIS	White Section <input checked="" type="checkbox"/>
DTIC	Gold Section <input type="checkbox"/>
DTIC SOURCE	
IDENTIFICATION	
DATE	
LOCATION/AVAILABILITY CODES	
DATE, CASE, SPECIAL	
A	

TABLE OF CONTENTS

	<u>Page</u>
ABSTRACT	i
FOREWORD	iii
LIST OF ILLUSTRATIONS	vii
LIST OF TABLES	ix
1. INTRODUCTION	1
2. MAGNETOMETER DATA	3
2.1 Location of Magnetometer Stations	3
2.2 Discussion of Magnetometer Data for the Three AEOLUS Rocket Launch Sets	7
2.2.1 Magnetically Active Launches - 10 April 1975	7
2.2.2 Magnetically Quiet Launches - 21 April 1975	18
2.2.3 Auroral Launches - 25 April 1975	23
3. ELECTROJET MODELS	23
3.1 Flat Earth Model	30
3.2 Cylindrical Earth Model	33
3.3 More General Electrojet Models	35
3.4 Induced Earth Current Considerations	36
4. ELECTROJET CALCULATIONS FOR THE AEOLUS LAUNCHES	43
4.1 Magnetically Active Launches - 10 April 1975	43
4.2 Magnetically Quiet Launches - 21 April 1975	56
4.3 Auroral Launches - 25 April 1975	56
5. SUMMARY OF MAGNETIC AND ELECTROJET CONDITIONS FOR THE AEOLUS LAUNCHES	59
5.1 Magnetically Active Launches - 10 April 1975	59
5.2 Magnetically Quiet Launches - 21 April 1975	60
5.3 Auroral Launches - 25 April 1975	60
6. CONCLUSIONS AND RECOMMENDATIONS	61
REFERENCES	63

LIST OF ILLUSTRATIONS

	<u>Page</u>
2. 1 Map Showing Locations of the Magnetometer Stations.	5
2. 2 Portion of Magnetometer Record from Ft. Churchill for the 10 April 1975 Launches.	8
2. 3 Portion of Magnetometer Record from Sitka for the 10 April 1975 Launches.	10
2. 4 Portion of Storm Magnetometer Record from College for the 10 April 1975 Launches.	11
2. 5 Portion of Magnetometer Record from Meanook for the 10 April 1975 Launches.	12
2. 6 Portion of Magnetometer Record from Ft. Smith for the 10 April 1975 Launches.	13
2. 7 Portion of Magnetometer Record from Great Whale River for the 10 April 1975 Launches.	14
2. 8 Portion of the Magnetometer Record from Cambridge Bay for the 10 April 1975 Launches.	15
2. 9 Portion of the Magnetometer Record from Newport for the 10 April 1975 Launches.	17
2. 10 Portion of Ft. Churchill Magnetometer Record for the 21 April 1975 Launches.	19
2. 11 Portion of Ft. Churchill Magnetometer Record Preceding the 21 April 1975 Launches.	20
2. 12 Portion of College Magnetometer Record for the 21 April 1975 Launches.	21
2. 13 Portion of the Great Whale River Magnetometer Record for the 21 April Launches.	22
2. 14 Portion of the Ft. Churchill Magnetometer Record for the 25 April 1975 Launches.	24
2. 15 Portion of the Leirvogur Magnetometer Record for the 25 April 1975 Launches.	25

LIST OF ILLUSTRATIONS (cont'd)

	<u>Page</u>
2. 16 Portion of the College Magnetometer Record for the 25 April 1975 Launches.	26
2. 17 Portion of the Great Whale River Magnetometer Record for the 25 April 1975 Launches.	27
2. 18 Portion of the Yellowknife Magnetometer Record for the 25 April 1975 Launches.	28
2. 19 Portion of the Ft. Smith Magnetometer Record for the 25 April 1975 Launches.	29
3. 1 Cross Section of Single Magnetometer Station Relative to the Auroral Electrojet.	31
3. 2 Geometry of the Electrojet Relative to a Single Magnetometer Station in a Cylindrical Earth Model.	34
3. 3 Geometry for the Induced Currents in a Cylindrical Earth with a Superconducting Shell at Depth H_0 .	38
3. 4 Variation of C_h and C_z in a Cylindrical Earth Model with a Superconducting Shell.	41
4. 1 Electrojet Parameters Calculated from the Ft. Churchill and O'Day Magnetometer Data for the Active Launches of 10 April 1975.	44
4. 2 Single Station Electrojet Map for 0925-0940 UT on 10 April 1975.	44
4. 3 Single Station Electrojet Map for 0945-1000 UT on 10 April 1975.	44
4. 4 Single Station Electrojet Map for 1005-1020 UT on 10 April 1975.	44
4. 5 Electrojet Parameters Calculated from the Ft. Churchill and O'Day Magnetometer Data for the Auroral Launches of 25 April 1975.	45

LIST OF TABLES

	<u>Page</u>
2.1 List of WDC-A Magnetometer Stations for Which Data have been Received.	4
2.2 List of Additional Magnetometer Stations for Which Data have been Received.	4
2.3 Listing of Magnetometer Station Data Coverage	6
2.4 K_p Indices for AEOLUS Launch Periods.	7
3.1 Comparison of Induced Current Effects in the Cylindrical Earth Model and the Field-Aligned Current Model.	40
4.1 Magnetic Disturbance Values for Several "Arcs" for the 10 April 1975 Event.	51
4.2 Electrojet Parameters for the Meanook "Arcs" for the 10 April 1975 Event.	52
4.3 Comparison of "Arc" Times at Meanook, Ft. Churchill, and Thompson, for the 10 April 1975 Event.	54
4.4 Calculated Arrival Times of Meanook "Waves" at Ft. Churchill for the 10 April 1975 Event.	55

1. INTRODUCTION

The AEOLUS (Auroral Excitation of Atmospheric Layers and Underlying Species) program involved the launch of three sets of three rockets each in April 1975 at Ft. Churchill, Manitoba, Canada. The main purpose of these launches was to study high altitude wave phenomena generated by auroral and magnetic disturbances. Two rockets in each set of three released puffs and trails of trimethylaluminum, which were illuminated by the sun in the first two launch sets. High altitude waves were to be detected by photographic study of the motion of the puffs and trails, with spectral data being used to attempt detection of thermal effects of these waves.

A real-time electrojet analysis instrument was used to assist in determining when conditions were suitable for the AEOLUS launches. This instrument was developed earlier to help determine if conditions were suitable for launch of rocket payloads designed to study the Auroral Electrojet (Refs. 1.1, 1.2 and 1.3). For the AEOLUS program the electrojet instrument was used to calculate approximate Auroral Electrojet parameters and thus help decide if conditions were suitable for launch. The electrojet parameters were calculated using a flat-earth model and using only an approximate correction for induced currents in the earth, but the results are sufficiently accurate to aid in the Auroral Electrojet conditions before and during an AEOLUS launch. Data from three axes magnetometers at Ft. Churchill and at O'Day Station about 130 km to the south were used to calculate the electrojet parameters.

The first rocket launch set was on 10 April 1975 during magnetically active conditions. Launch was during the morning twilight window when the high altitude chemical releases were illuminated by the sun, but the lower atmosphere was not and so Rayleigh scattered light did not obscure the releases. The electrojet instrument calculations showed a moderately intense electrojet some 100-200 km south of the chemical release area for about

20 minutes before launch of the first rocket. This indicated that conditions were reasonably good for detection of electrojet-generated high altitude waves, and so contributed significantly to the launch decision.

The second rocket launch set was on 21 April 1975 during magnetically quiet conditions, and during the morning twilight window. For this launch set the electrojet instrument established reasonable upper limits to the electrojet intensity, and so contributed in a minor way to the launch decision. This launch set was primarily as a background check for the magnetically active launch set, and the decision was based primarily on minimal activity of the magnetometers for some hours before launch.

The final rocket launch set was on 25 April 1975 during active auroral conditions with some associated magnetic activity. The launch was during the night and so did not provide as complete a set of data on the chemical releases as the twilight launches. Since auroral conditions were required for launch, the electrojet instrument contributed minimally to the actual launch decision, although the electrojet calculations are useful subsidiary data.

Subsequent to the AEOLUS launches additional magnetometer data for 22 stations within a few thousand km of Ft. Churchill have been obtained. These data define the magnetic, and hence electrojet, conditions in the Ft. Churchill region more precisely. A brief discussion of these data was given in Ref. 1.4. Here a more thorough discussion and analysis of these data is given. Effort has been concentrated on the magnetically active launch of 10 April, since that is the launch set most likely to detect high altitude waves. The quiet launch of 21 April requires little analysis, other than demonstration of the widespread magnetically quiet conditions. The auroral launch of 25 April, being a nighttime launch set, did not yield as much data as the twilight launches, and so is not heavily emphasized. However, the associated magnetic activity is briefly discussed, and some electrojet analysis is also given.

The magnetometer data are presented and discussed in Section 2. This is an expansion of the preliminary presentation given in Ref. 1.4. The electrojet models used for the analysis, as well as more advanced models currently being discussed in the literature, are described in Section 3. The electrojet instrument uses a flat-earth model, and this model has been modified to include a cylindrical-earth effect for the multi-station large area analyses. The electrojet calculation results are then presented in Section 4, and an overall summary of magnetic conditions for each of the three AEOLUS launch sets is given in Section 5. Conclusions and Recommendations are given in Section 6.

2. MAGNETOMETER DATA

2.1 Location of Magnetometer Stations

Data from 22 magnetometer stations have been obtained for the April 1975 AEOLUS launch periods. Not all stations have complete data coverage. The World Data Center A (WDC-A) for Solar Terrestrial Physics, Boulder, Colorado, supplied data for 16 stations listed in Table 2.1. Ft. Churchill data were also obtained from the real-time print-outs of the electrojet instrument. Data from a magnetometer station at Ft. Smith (first entry in Table 2.2) were obtained from Gordon Rostoker of the University of Alberta, while that from four additional stations near Ft. Churchill were obtained from John Walker of the Dept. of Energy, Mines, and Resources, of Canada (middle entries in Table 2.2). The last entry in Table 2.2 is for O'Day Station for which partial coverage was obtained from the electrojet instrument print-outs.

The locations of the stations are shown in Fig. 2.1, with each station identified by its 2- or 3-letter code from Tables 2.1 and 2.2. The station data coverage for the AEOLUS launches is given in Table 2.3. Most stations have complete coverage for all three (HDZ or XYZ) magnetometer components.

Table 2.1

List of WDC-A Magnetometer Stations for Which Data have been Received

<u>Station</u>	<u>Symbol</u>	<u>Geographic</u>	<u>Geomagnetic</u>
		<u>Lat (deg N)/Long (deg W)</u>	<u>Lat (deg N)/Long (deg E)</u>
Fort Churchill	CHR	58.8/94.1	68.8/322.5
Yellowknife	YK	62.5/114.5	69.1/292.6
Meanook	ME	54.6/113.3	61.8/301.0
Sitka	SI	57.1/135.3	60.1/275.9
College	CO	64.9/147.8	64.7/257.0
Cambridge Bay	CB	69.1/105.0	76.7/294.0
Baker Lake	BL	64.3/96.0	73.9/314.8
Mould Bay	MLB	76.2/119.4	79.1/284.7
Resolute	RB	74.7/94.9	83.1/287.7
Great Whale River	GW	55.3/77.8	66.8/347.2
St. John	JO	47.6/52.7	58.7/21.4
Ottawa	OT	45.4/75.6	57.0/351.5
Newport	NPT	48.3/117.0	55.2/300.8
Victoria	VI	48.5/123.4	54.3/292.7
Narssarssuaq	NQ	61.2/45.4	71.1/37.4
Leirvogur	RY	64.2/21.7	70.1/71.5

Table 2.2

List of Additional Magnetometer Stations for Which Data have been Received

<u>Station</u>	<u>Symbol</u>	<u>Geographic</u>	<u>Geomagnetic</u>
		<u>Lat (deg N)/Long (deg W)</u>	<u>Lat (deg N)/Long (deg E)</u>
Fort Smith	FSM	60.0/112.2	67.3/299.7
Winnipeg	WPG	49.6/97.1	59.4/323.8
Thompson	TMP	55.8/97.8	65.4/319.3
Eskimo Point	EP	61.1/94.1	71.1/321.8
Rankin Inlet	RI	62.8/92.3	72.9/321.9
O'Day Station	OD	57.6/94.2	64.4/322.3



Fig. 2.1 Map Showing Locations of the Magnetometer Stations.

Table 2. 3

Listing of Magnetometer Station Data Coverage

Station Symbol	Data for AEOLUS launches of 1975*		
	10 April	21 April	25 April
CHR	N	N	N
YK	N	N	N
ME	N	N	N
SI	N	N	N
CO	N, S	N, S	N
CB	N	N	N
BL	(U)	N	N
MLB	N	N	N
RB	N	N	N
GW	N	N	N
JO	N	N	N
OT	N	N	N
NPT	N	N	N
VI	N	N	N
NQ	N	N	N
RY	N	N	N
FSM	N	N	N
WPG	N	N	N
TMP	N	N	N
EP	(PZ)	(PZ)	(PZ)
RI	-	(PD)	(PD)
OD	(P)	(P)	(P)

*N = normal, S = storm, (U) = unusable,
 (PZ) = Z component missing, (PD) = D component missing, - = no data received,
 (P) = partial coverage.

The three-hourly K_p indices are listed in Table 2.4 for three day periods centered on the day of each rocket launch set. The bracketed K_p value is for the actual launch period.

Table 2. 4
Kp Indices for AEOLUS Launch Periods

Date in April 1975	Three-hour range indices, Kp							
	<u>1</u>	<u>2</u>	<u>3</u>	<u>4</u>	<u>5</u>	<u>6</u>	<u>7</u>	<u>8</u>
9	5-	6	5	4+	4	6	5-	6-
10	5+	5	4	[4+]	4	3+	4	5
11	5+	5	4	5-	5	4	3-	3+
20	0+	1-	2	2+	3	5-	6-	5+
21	6	2+	2	[3]	4	4-	3+	1+
22	3+	4	3+	2	3-	2	3-	4-
24	4	3	3	4	2+	3	3	3
25	3-	[3-]	2+	2-	2-	2-	1-	2-
26	4-	1+	1	2+	2-	2+	3-	2

Note: three-hour period for each rocket launch set is shown in brackets.

2. 2 Discussion of Magnetometer Data for the Three AEOLUS Rocket Launch Sets

2. 2. 1 Magnetically Active Launches - 10 April 1975

The first set of three rockets was launched during the dawn window on 10 April 1975. The first rocket was launched at 0954 UT, and started the magnetically active launch set. The indices in Table 2.4 show that K_p was 4+, and that K_p had averaged near 5 for the preceding 24 hours.

A survey of the magnetometer data from the stations in Tables 2.1 and 2.2 shows periods of strong activity for 0130 to 0500 UT, 0700 to 0830 UT, and 0930 to 1230 UT. The magnetometer data from Ft. Churchill for 0630 to 1400 UT are shown in Fig. 2.2. The X-component shows a moderately sharp step at 0923 UT, and a stronger, sharper step at 0940 UT, and the second at 1140 UT. Activity occurred in two periods, the first peaking at 1003 UT, and the second at 1140 UT.

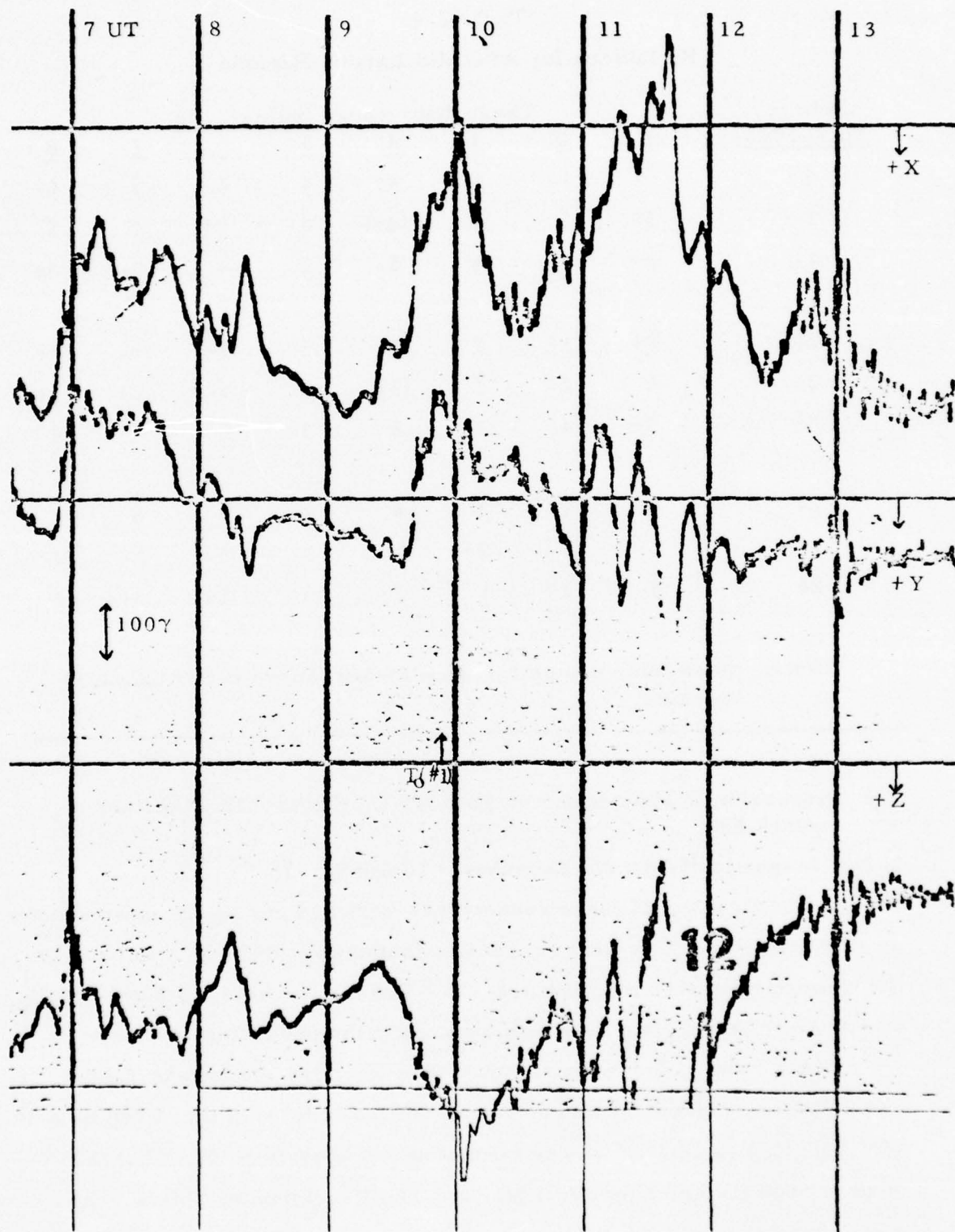


Fig. 2.2 Portion of Magnetometer Record from
Ft. Churchill for the 10 April 1975 Launches.

The magnetometer data from Sitka are shown in Fig. 2.3. The activity before 0909 UT is not as strong as at Ft. Churchill, but the peaks at 0931 and 1214 in H are comparable in magnitude to the Ft. Churchill X disturbance. The College storm magnetometer data in Fig. 2.4 show a similar variation, and together with Sitka show a strong substorm from 0909 to 0949 centered over Alaska and northwestern Canada.

The data from Meanook in Fig. 2.5 show the same trend in the H component, although the timing is slightly later than at College and Sitka. This is even more pronounced for the Ft. Smith data in Fig. 2.6, where the H component peaks after 1000 UT, more in agreement with Ft. Churchill. The substorm thus appears to have started over Alaska and northwestern Canada, and traveled eastward toward Ft. Churchill. The disturbance did not reach very far east of Ft. Churchill, since the magnetometer data from Great Whale River (Fig. 2.7) show no strong negative H disturbance as at Ft. Churchill, although there is some activity present.

An interesting feature is the approximately five minute periodicity, or pulsation, in the X(H) component at some of the magnetometer stations. This is most obvious in the Meanook data (Fig. 2.5), and also in the Ft. Churchill data (Fig. 2.2).

The 10 April disturbance thus appears to have started west of Ft. Churchill at about 0900 UT, peaked in the west at 0930-0945 UT, and ended near 1000 UT. Near Ft. Churchill the disturbance started near 0920 UT, peaked at about 1005 UT, and ended near 1030 UT. A second disturbance commenced almost immediately, peaked near 1145 UT, and ended near 1230 UT.

The disturbance as it appeared in more polar stations is shown by the Cambridge Bay data in Fig. 2.8. The large positive Z component shows a strong westward electrojet to the south, peaking at about 0955 and 1005 UT. The event appears to have started at 0925 UT, with the major intensification beginning about 0940 UT. Mould Bay shows structure similar

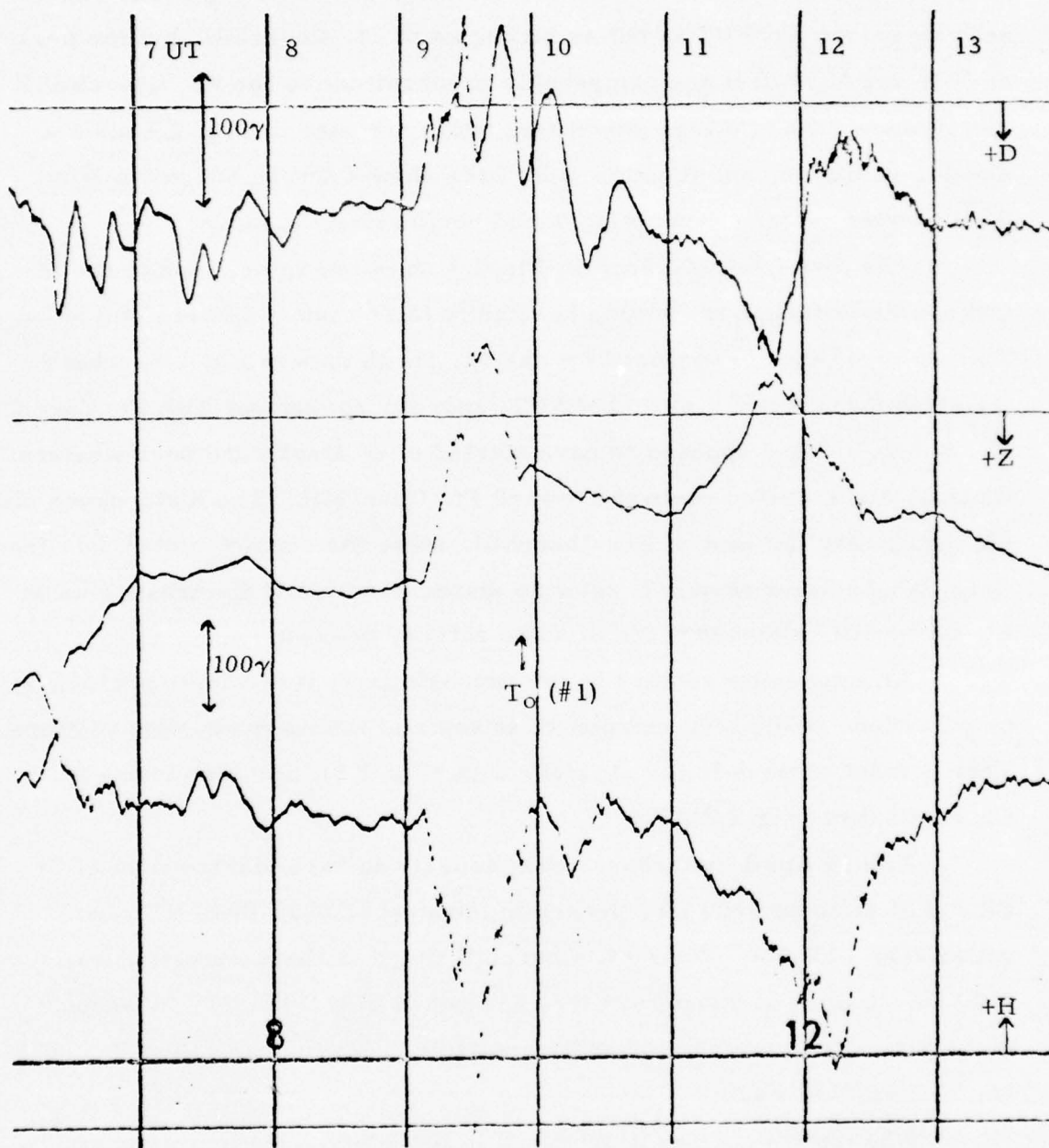


Fig. 2. 3. Portion of Magnetometer Record from Sitka for the 10 April 1975 Launches.

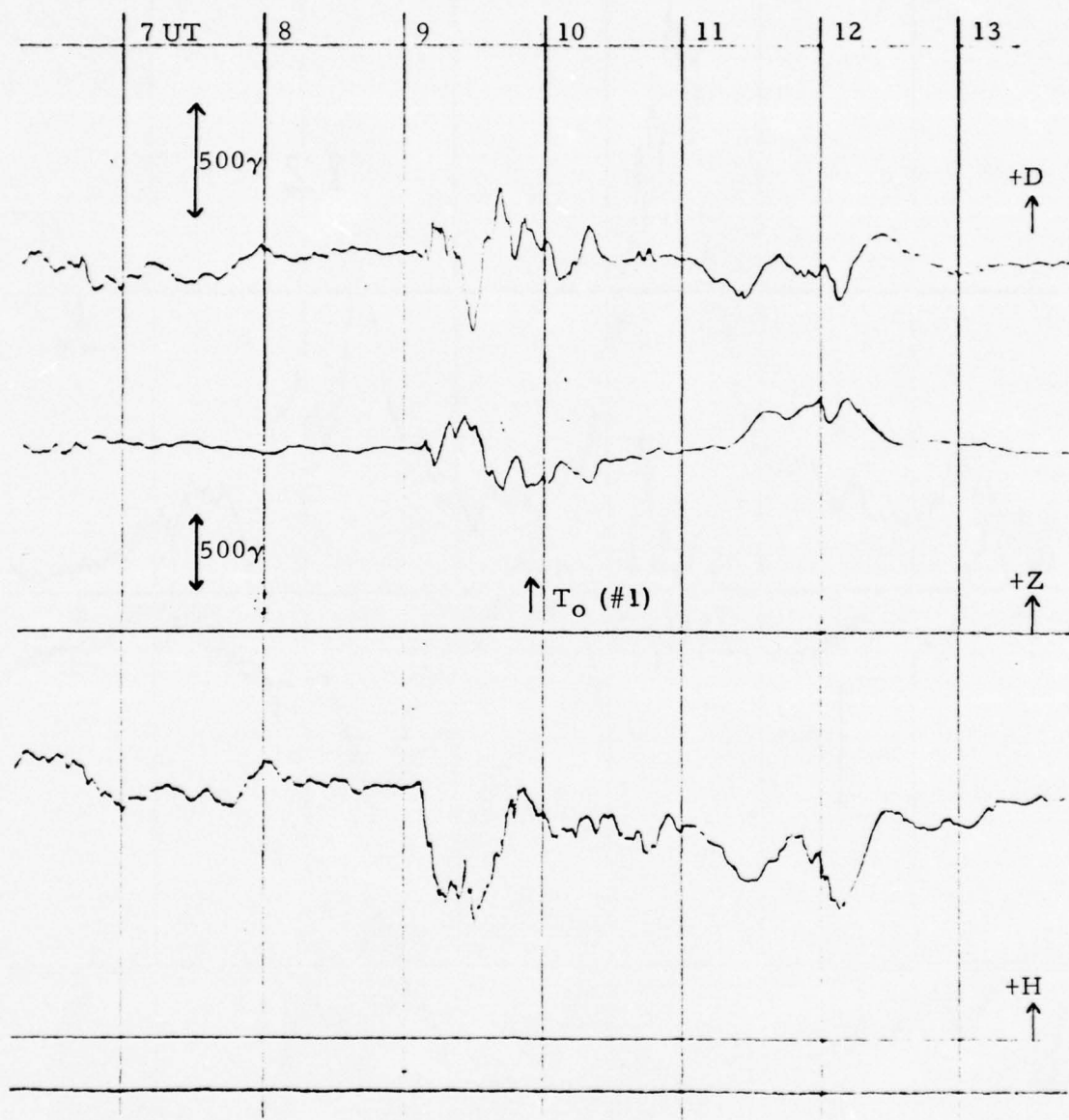


Fig. 2.4. Portion of Storm Magnetometer Record from College for the 10 April 1975 Launches.

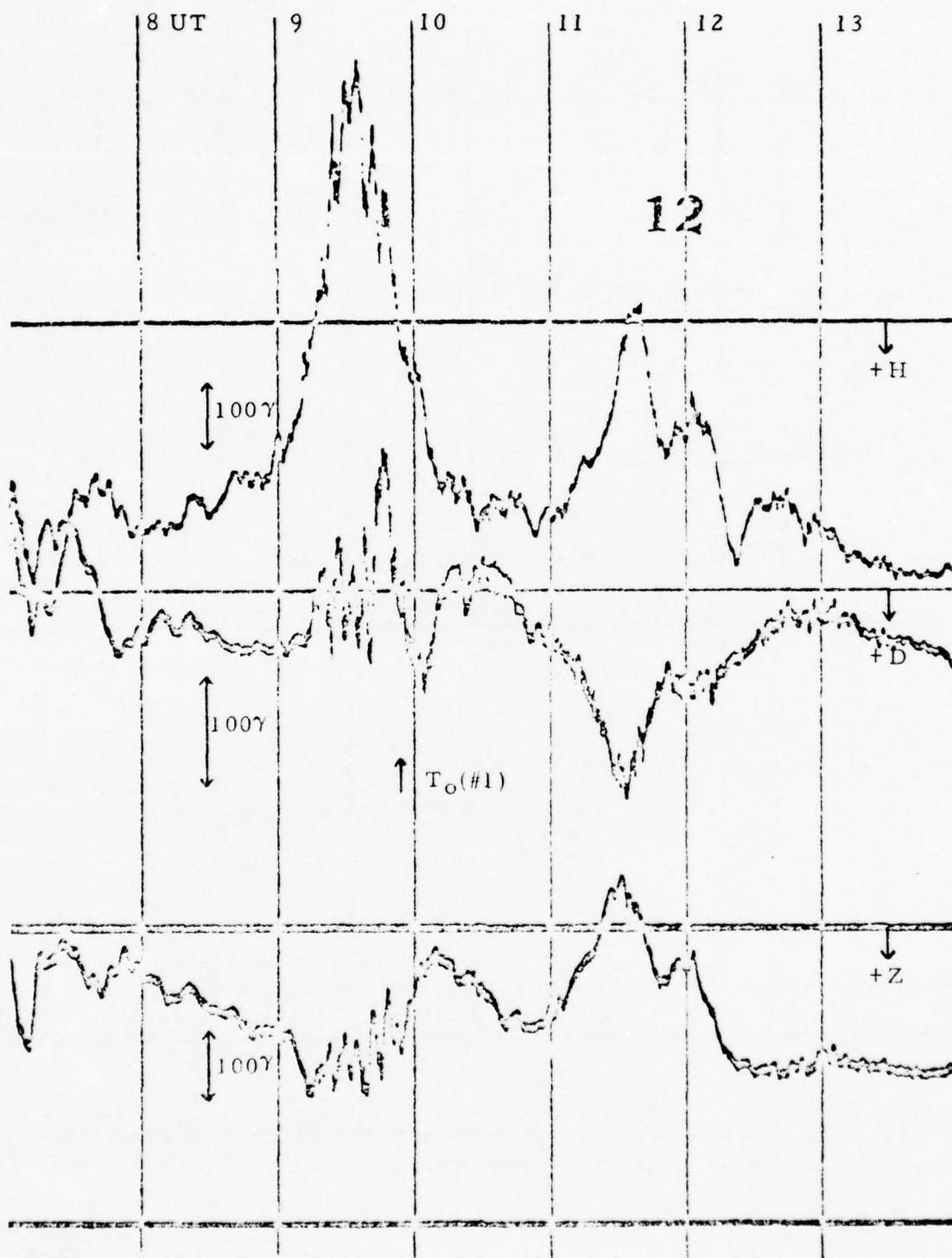


Fig. 2.5 Portion of Magnetometer Record from Meanook for the 10 April 1975 Launches.

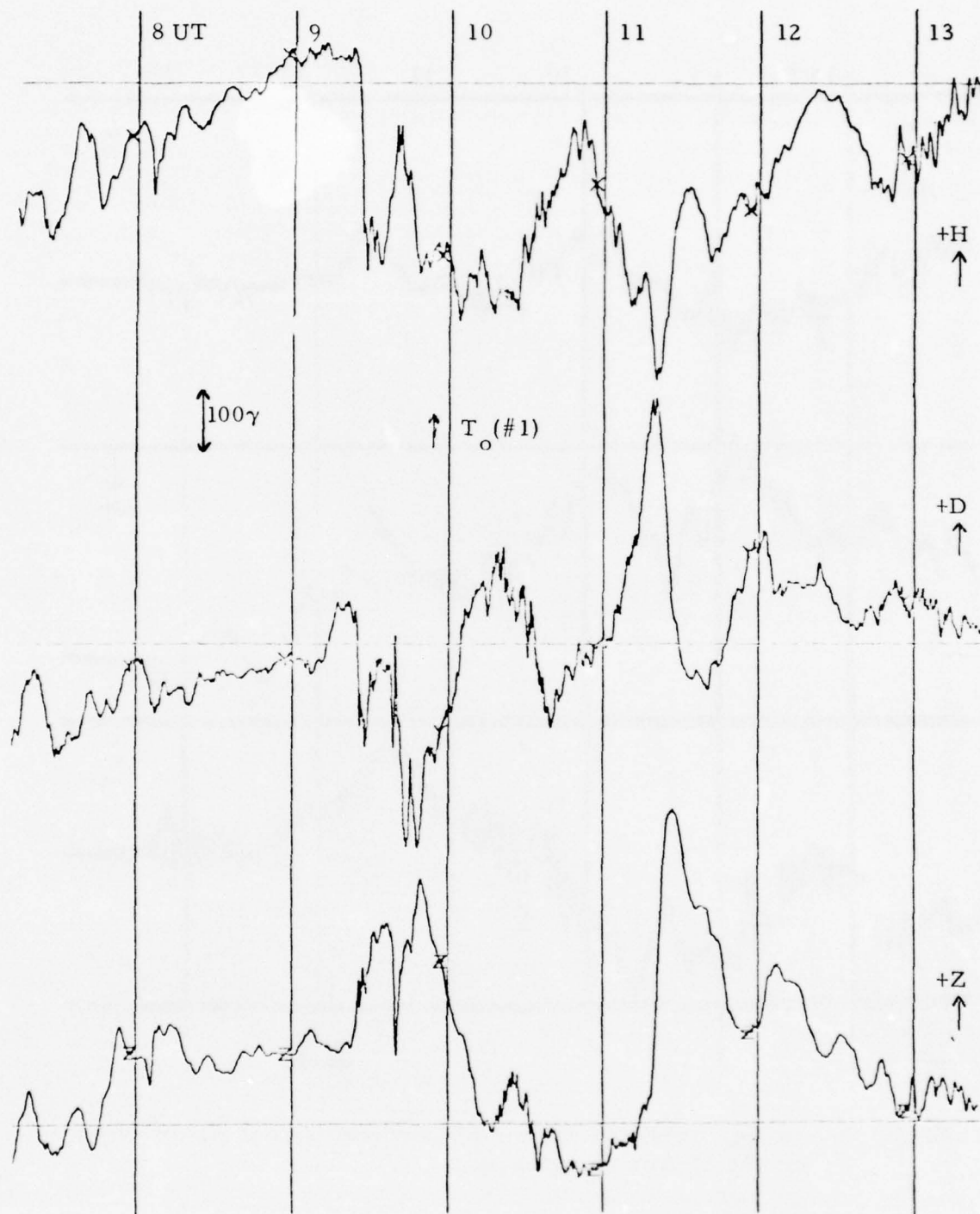


Fig. 2. 6. Portion of Magnetometer Record from Ft. Smith for the 10 April 1975 Launches.

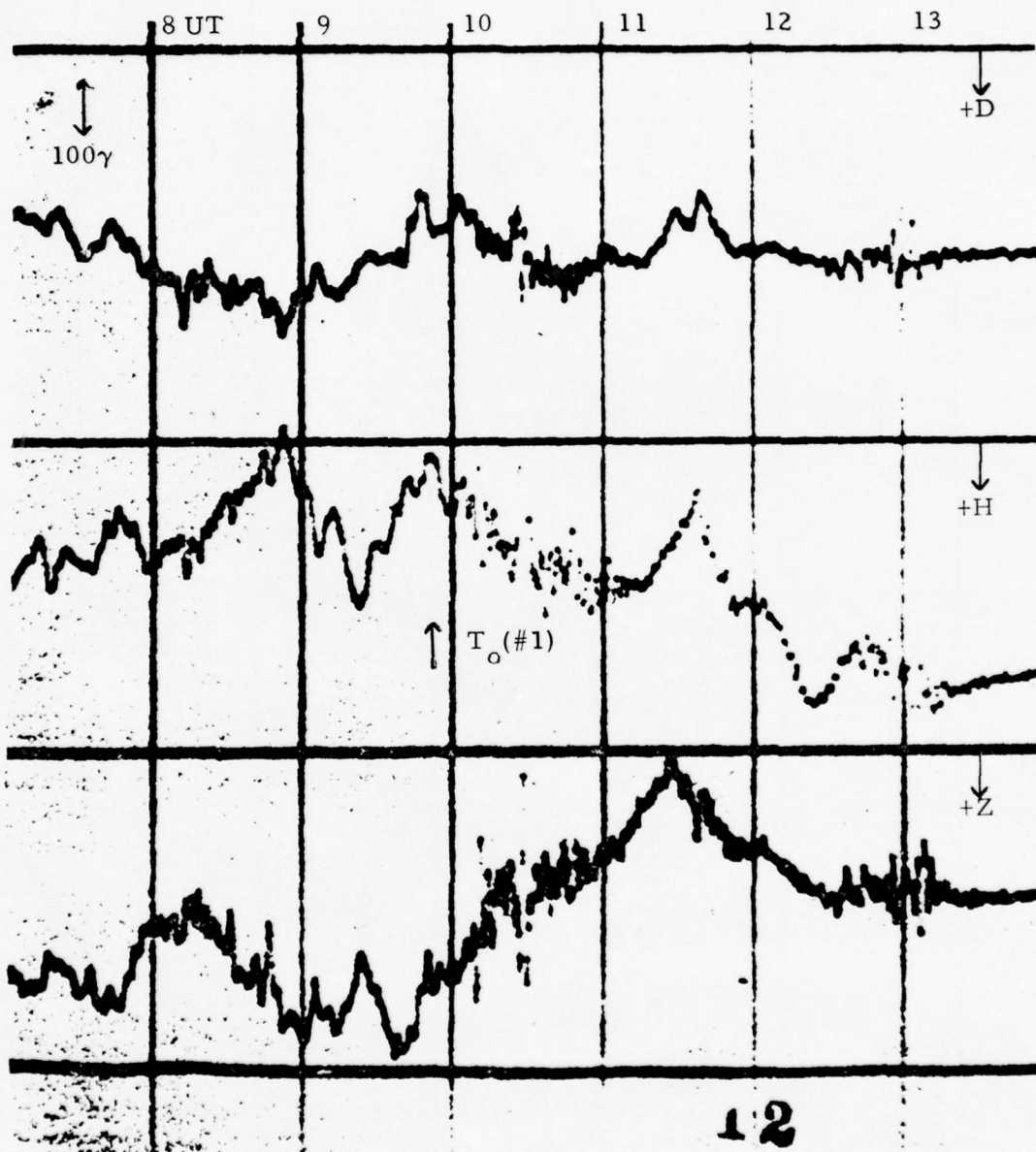


Fig. 2.7. Portion of Magnetometer Record from Great Whale River for the 10 April Launches.

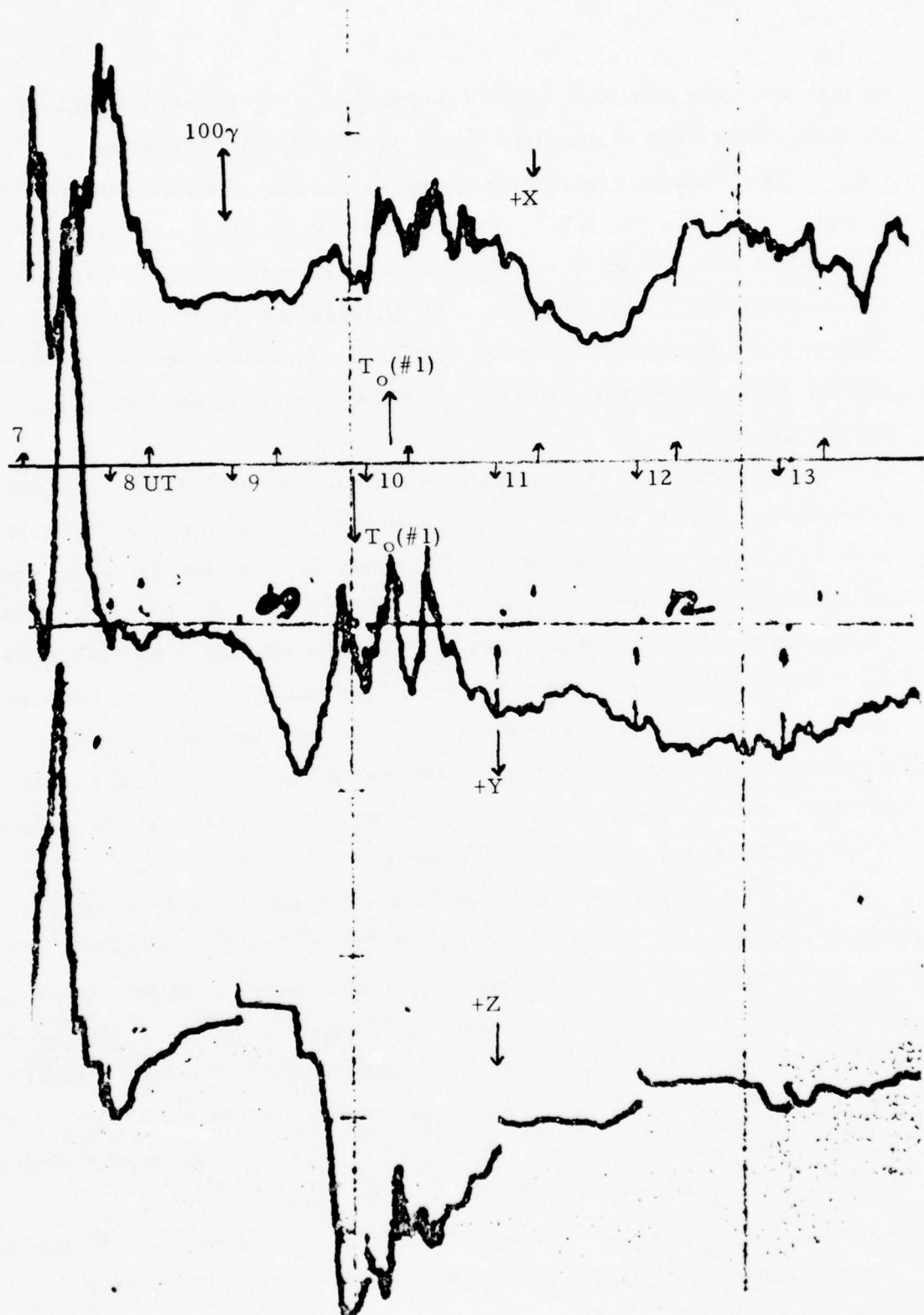


Fig. 2.8 Portion of Magnetometer Record from Cambridge Bay for the April 1975 Launches.

to that at Cambridge Bay, while Resolute has a significantly weaker Z response with most of the disturbance being in the Y component.

The southern region magnetometer response is shown by the Newport record in Fig. 2.9. A mild negative Z, peaking near 0945 UT, is present, and activity in the D component is somewhat larger than in the H component. The disturbance at Victoria is quite similar to that at Newport, as is the disturbance at Winnipeg. The disturbances at Ottawa and St. John are weaker, with Ottawa showing most of the disturbance in the D component.

The remaining stations can be summarized as follows. Yellowknife is similar to Ft. Smith, while Baker Lake, although mostly unreadable, appears similar to Ft. Churchill. Thompson is also similar to Ft. Churchill except for the sign of the Z component, which places the electrojet between Thompson and Ft. Churchill. The H and D components at Eskimo point (no Z was recorded) are similar to Ft. Churchill while no data were obtained for Rankin Inlet (see Table 2.3). O'Day is also similar to Ft. Churchill. The disturbances at Narssarssuaq and Leirvogur are both similar, showing only minor, irregular variations, and thus indicating no electrojet far to the east of Ft. Churchill.

The 10 April disturbance can be broken down into three sections of minor activity, from about 0925-0940 UT, 0945-1000 UT, and 1005-1020 UT. For the first period the activity was primarily from Ft. Smith westward to College, with only weak activity near Ft. Churchill. The activity then moved to the Ft. Churchill to Ft. Smith region for the second period, with little activity to the west. Finally the third period showed strong activity from Ft. Churchill (perhaps also Great Whale River) all the way west to College. These three periods will be analyzed in more detail in Section 4 where electrojet maps will be given. After 1020 UT this event decayed, with a second event starting near 1040 UT and peaking at 1100-1200 UT. This second event is of only minor interest for the AEOLUS program, since it could have no influence on the much earlier rocket launch data.

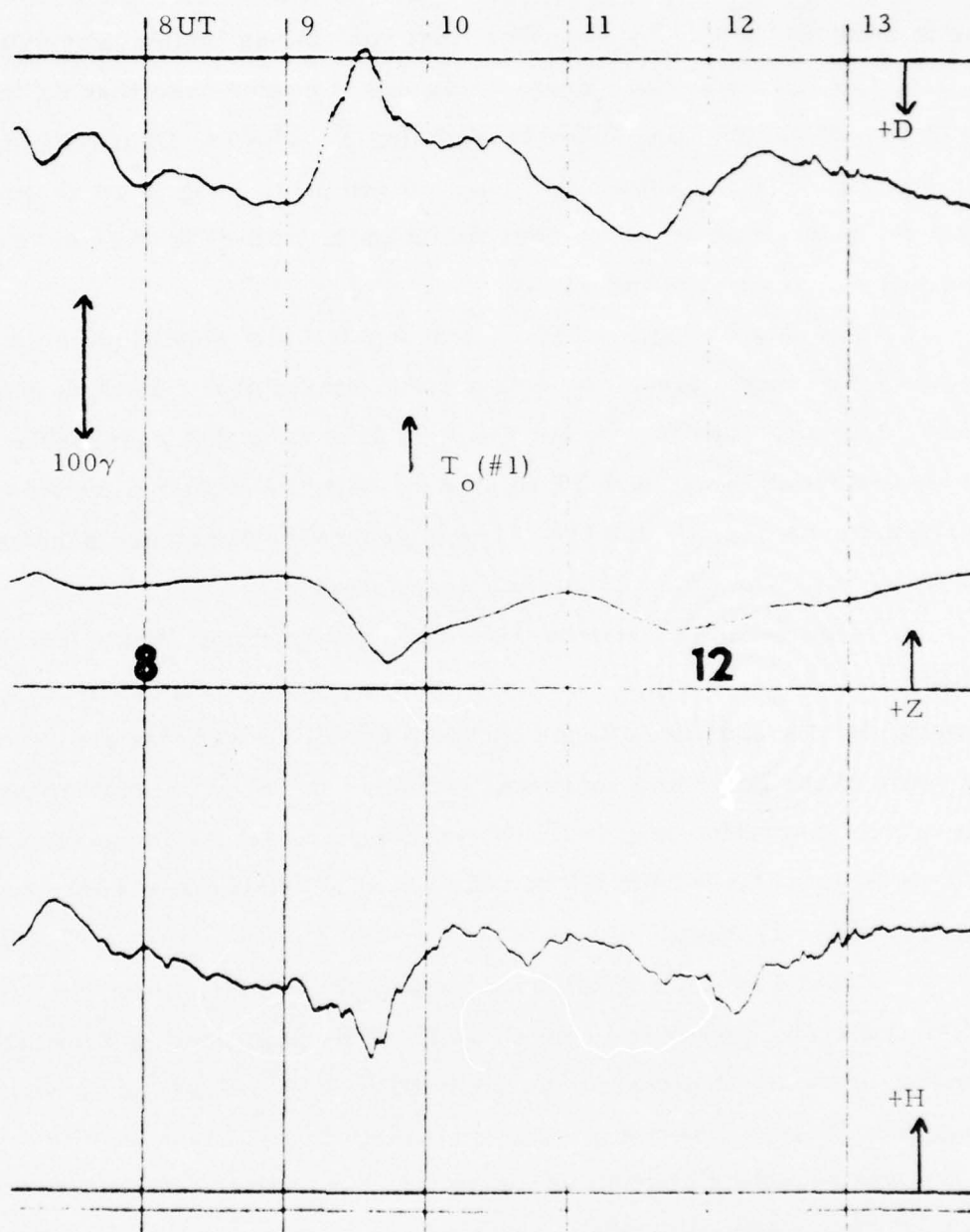


Fig. 2.9 Portion of Magnetometer Record for Newport for the 10 April 1975 Launches.

2.2.2 Magnetically Quiet Launches - 21 April 1975

The second set of three rockets was launched during relative magnetic calm on 21 April 1975. The first rocket was launched at 0907 UT during the dawn window. From Table 2.4 it can be seen that K_p was 3, with the preceding three-hour index being 2. The Ft. Churchill magnetometer records are shown in Figs. 2.10 and 2.11. Fig. 2.10 shows the activity before and after the rocket launches, while Fig. 2.11 shows the activity for several hours earlier.

The data in Fig. 2.10 show reasonably quiet conditions before launch up to an hour after launch. Some activity starts near 1030 UT, peaking near 1230 and 1400 UT. From Fig. 2.11 it is seen that reasonable quiet prevailed from about 0400 UT to launch, with the most recent strong disturbance centered on 0200 UT. These general features are present in the records of all the other magnetometer stations.

Magnetometer records from College and Great Whale River are shown in Figs. 2.12 and 2.13. Both show a small (about 50 γ peak-to-peak amplitude) oscillation centered on about 0850 UT, and this also shows up in some of the polar and southern stations. At Ft. Churchill this shows up as a 20 γ negative step in the X component. More intense activity is absent from at least 0400 UT to 1000 UT at all stations in Table 2.3 which have data for 21 April.

From Table 2.4 it can be seen that for 6 hours before to three hours after launch K_p was in the range 2 to 3. This plus the data from the magnetometer stations, illustrated by that in Figs. 2.10 to 2.13, show that extreme magnetic quiet was not present for the 21 April launches. However, there was complete absence of substorms for a period of 5 hours before to 1-1/2 hours after the first launch. This launch set thus sampled an upper atmosphere undisturbed by electrojet produced waves.

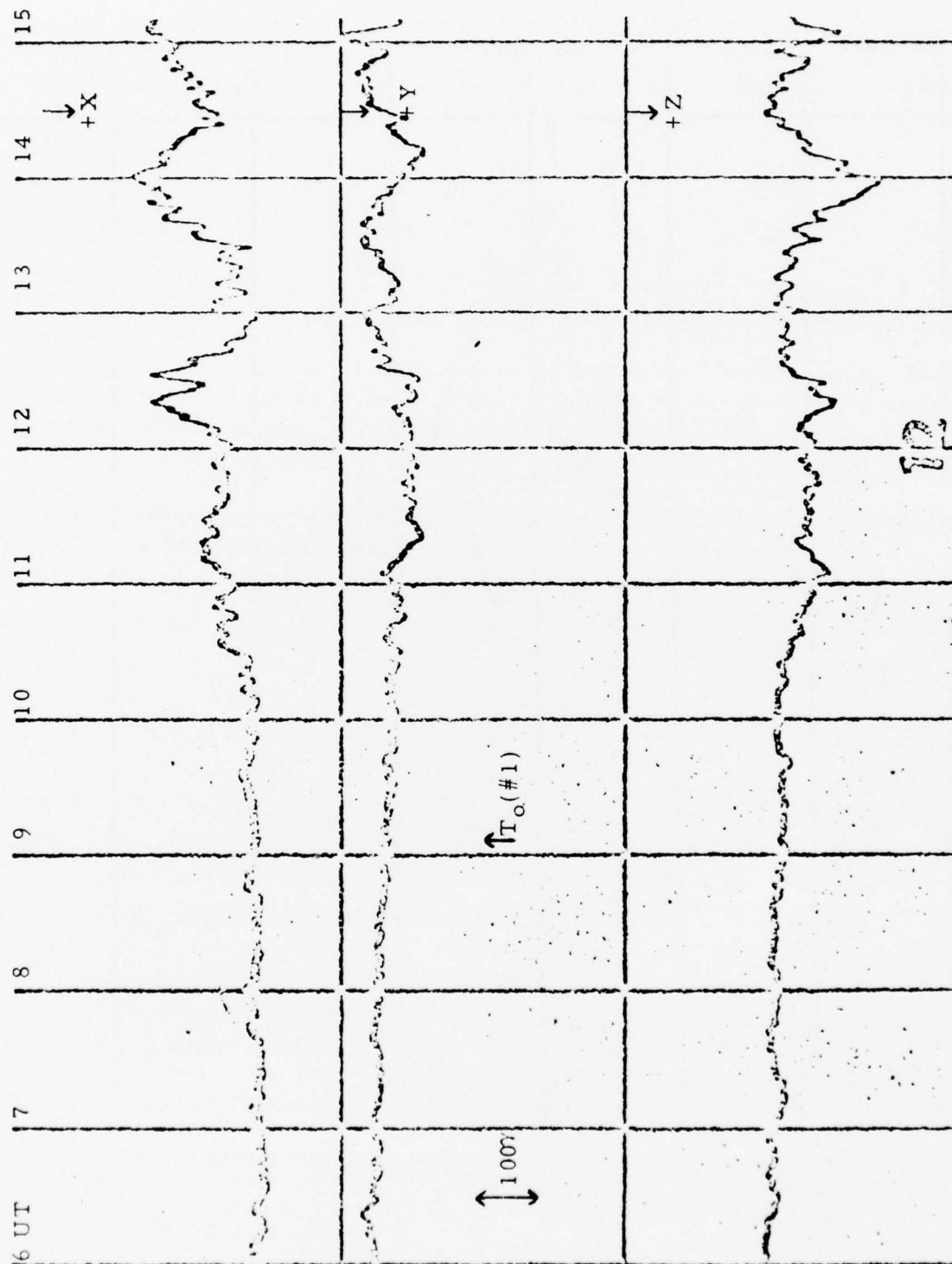


Fig. 2.10 Portion of Ft. Churchill Magnetometer Record for the 21 April 1975 Launches.

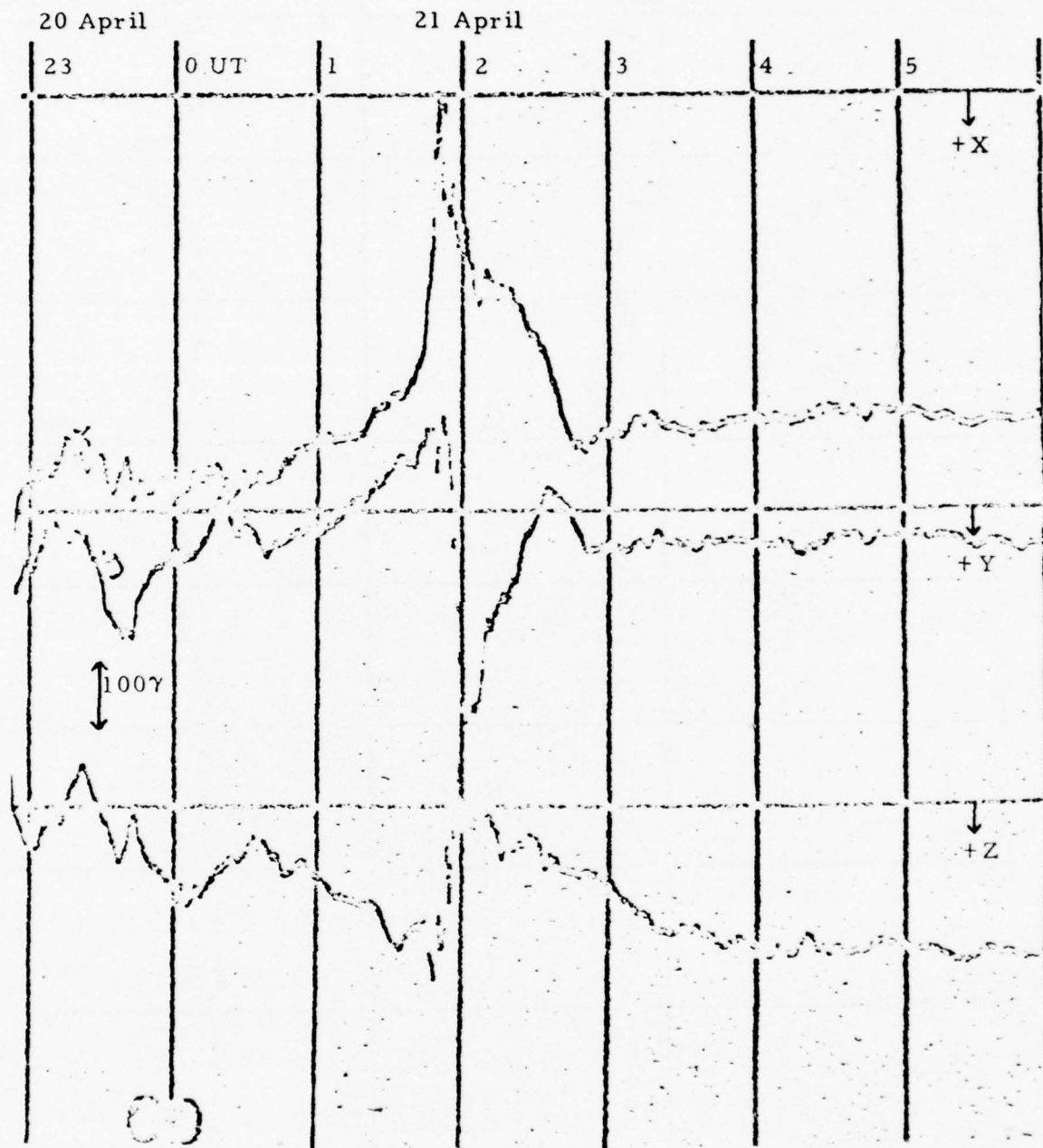


Fig. 2.11 Portion of Ft. Churchill Magnetometer Record
Preceding the 21 April 1975 Launches.

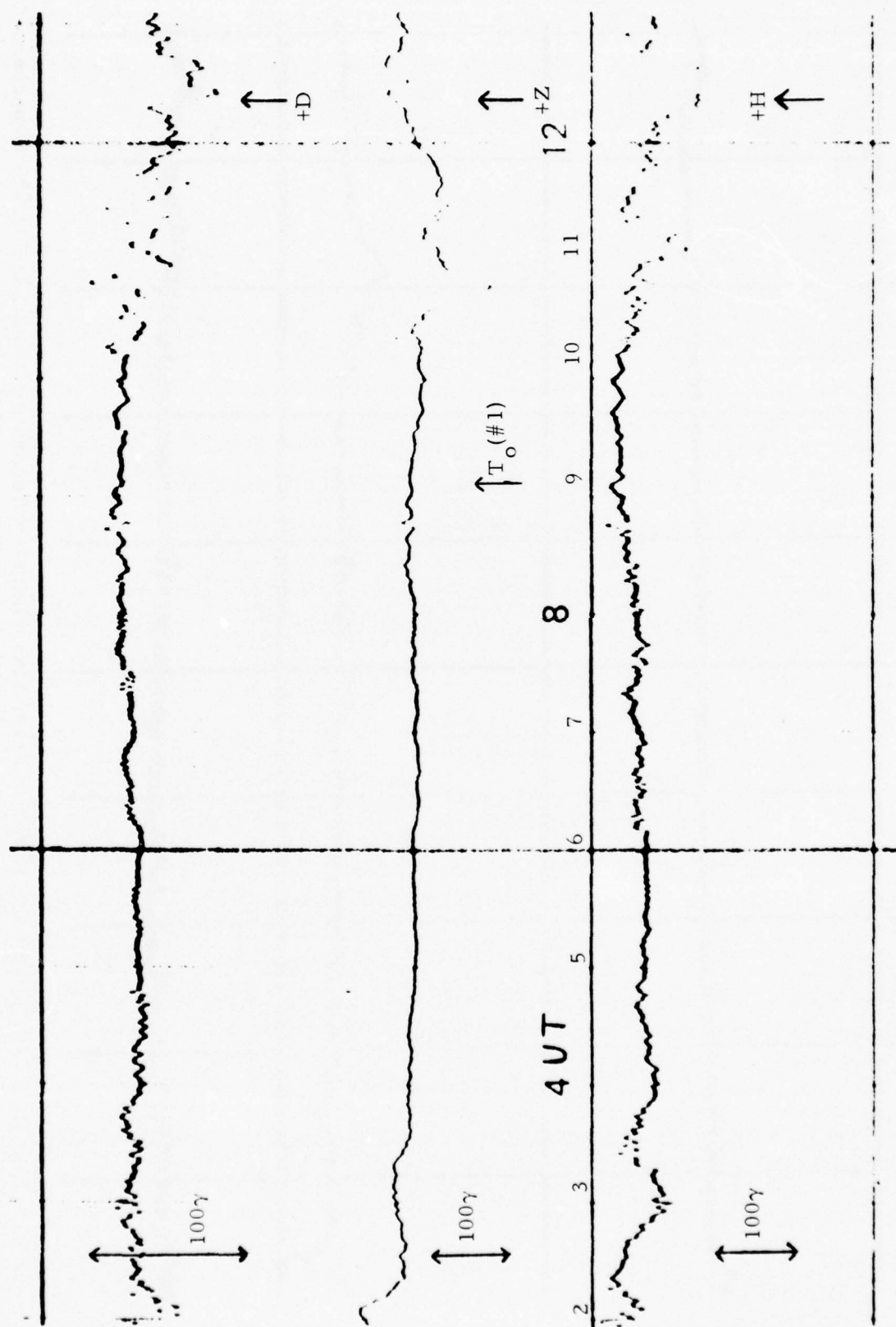


Fig. 2.12 Portion of College Magnetometer Record for the 21 April 1975 Launches.

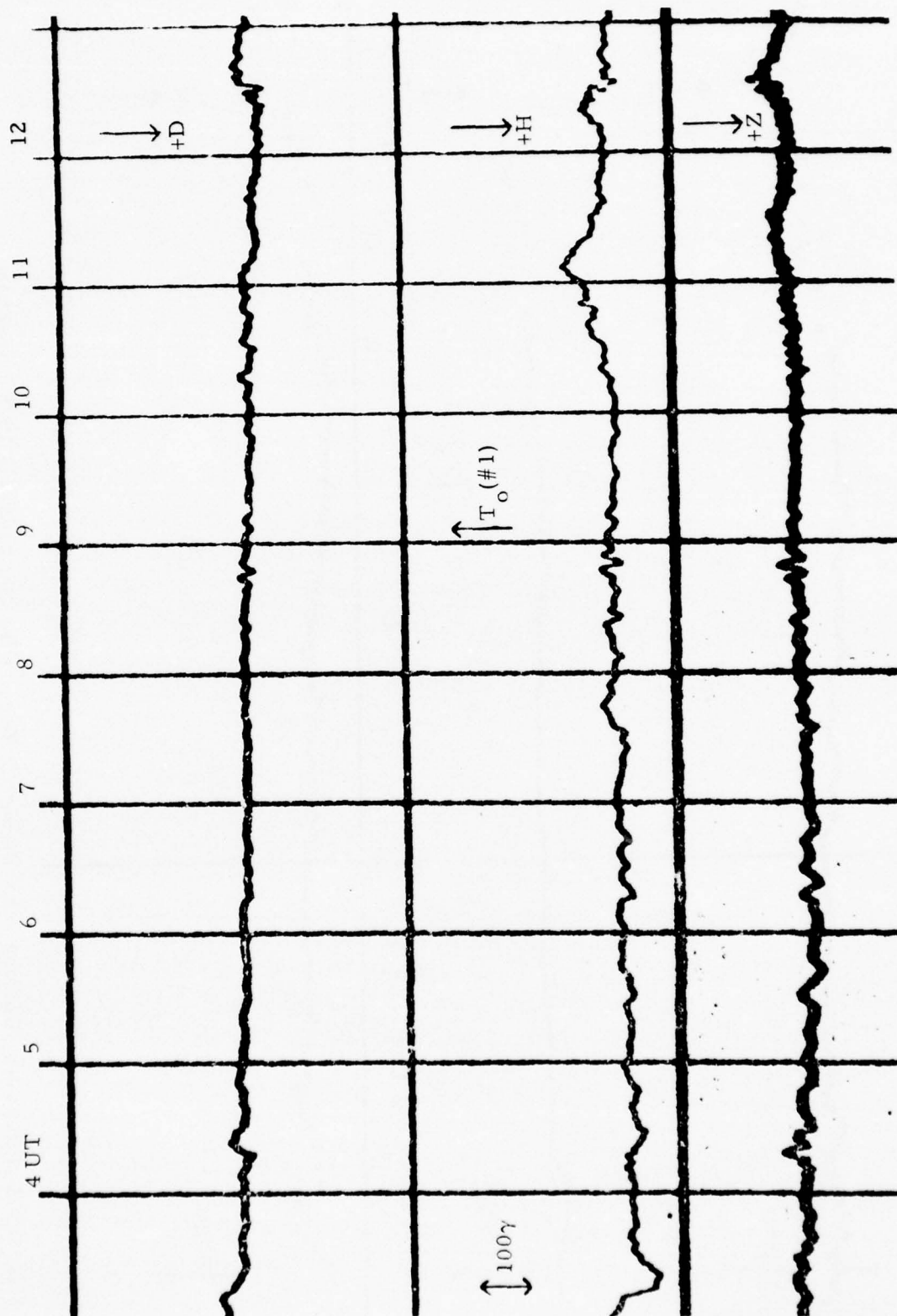


Fig. 2.13 Portion of Great Whale River Magnetometer Record for the 21 April 1975 Launches.

2.2.3 Auroral Launches - 25 April 1975

The third set of three rockets was launched into an active auroral display on 25 April 1975. The first rocket was launched at 0413 UT, about two hours before local midnight. From Table 2.4 it is seen that conditions were only moderately active magnetically, with $K_p=3-$. The Ft. Churchill magnetometer record for this period is shown in Fig. 2.14. The Ft. Churchill data show good magnetic activity before and after the rocket launches. Other stations show general agreement in the timing, with the activity being broadly centered near Ft. Churchill.

The extent of the activity in longitude is shown by the Leirvogur and College data in Figs. 2.15 and 2.16. The Great Whale River magnetometer data in Fig. 2.17, the Yellowknife data in Fig. 2.18, and the Ft. Smith data in Fig. 2.19 show that the most intense activity was at Ft. Churchill and somewhat to the east.

The variations in the Ft. Churchill Z component in Fig. 2.14 show that the electrojet started to the south and moved north over Ft. Churchill about 10 minutes after launch of the first rocket. The X component shows a large amount of pulsation with a rough 5 minute period, so upper atmosphere waves may be present. The closeness of the generation region to Ft. Churchill may, however, make the wave motion near Ft. Churchill more complex, and a simple 5 or so minute period sinusoid may not be present.

The magnetic activity for the auroral launches was not as intense as that for the magnetically active launches of 10 April, nor was it as well suited for possible upper atmosphere wave generation. The activity was centered near Ft. Churchill, so some strong, irregular wave motion may be observable in the chemical release observations.

3. ELECTROJET MODELS

The electrojet instrument was originally designed to aid in rocket launches intended to go near the Auroral Electrojet. Thus it was of most use for nearby electrojets, and the flat earth, infinite line current model

BEST AVAILABLE COPY

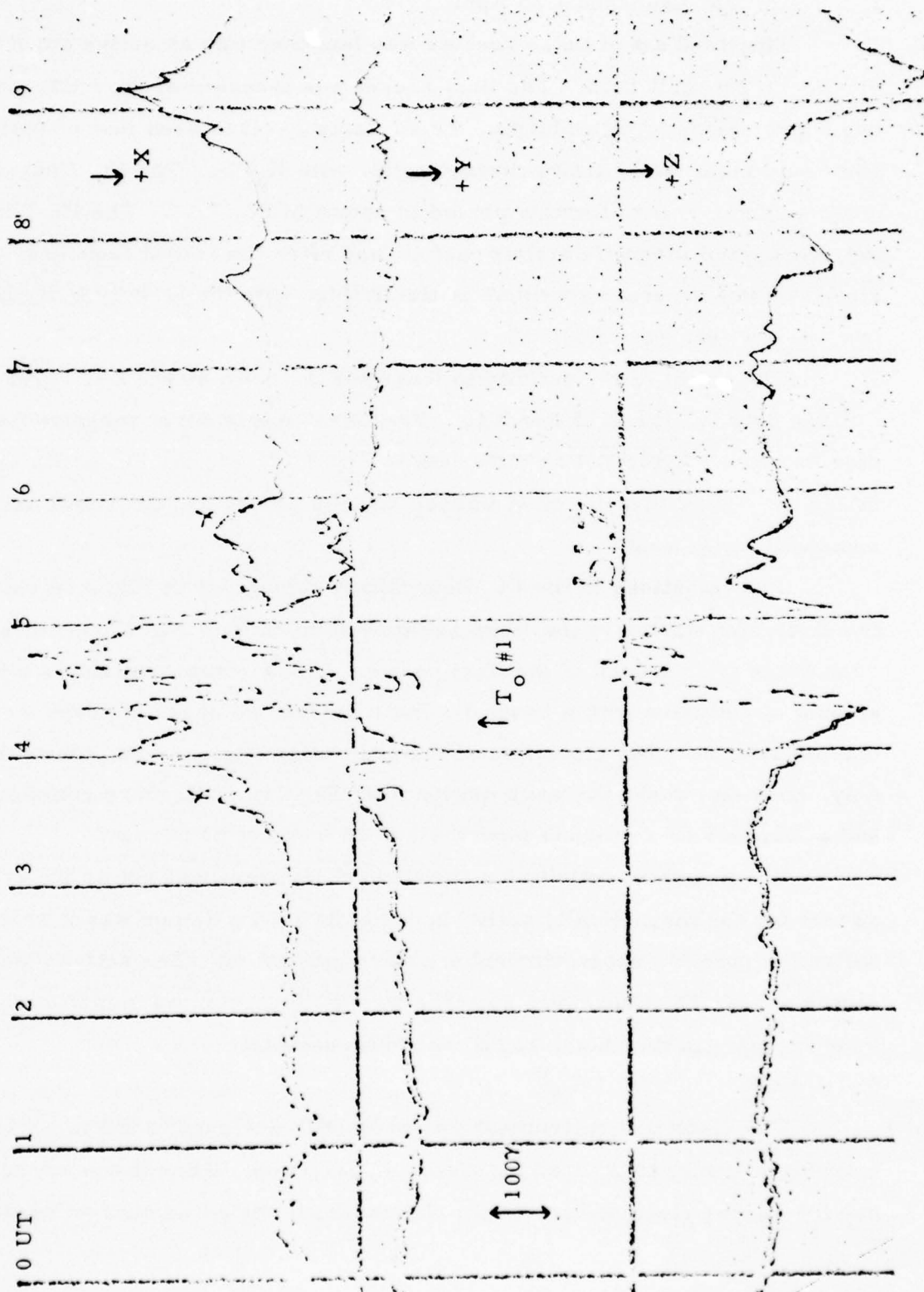


Fig. 2. 14 Portion of the Ft. Churchill Magnetometer Record for the
25 April 1975 Launches.

BEST AVAILABLE COPY

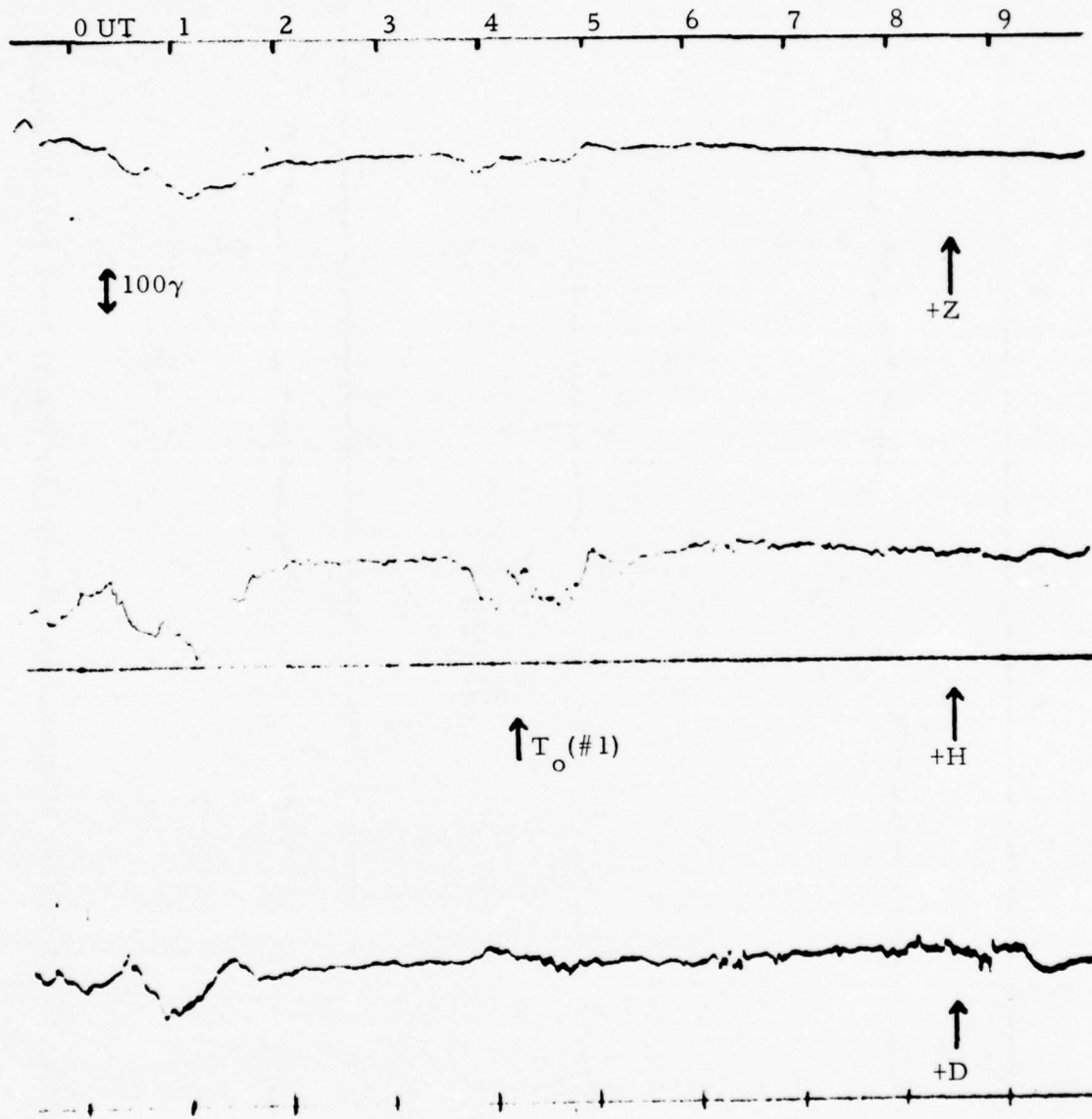


Fig. 2. 15 Portion of the Leirvogur Magnetometer Record for the 25 April 1975 Launches.

BLE COPY

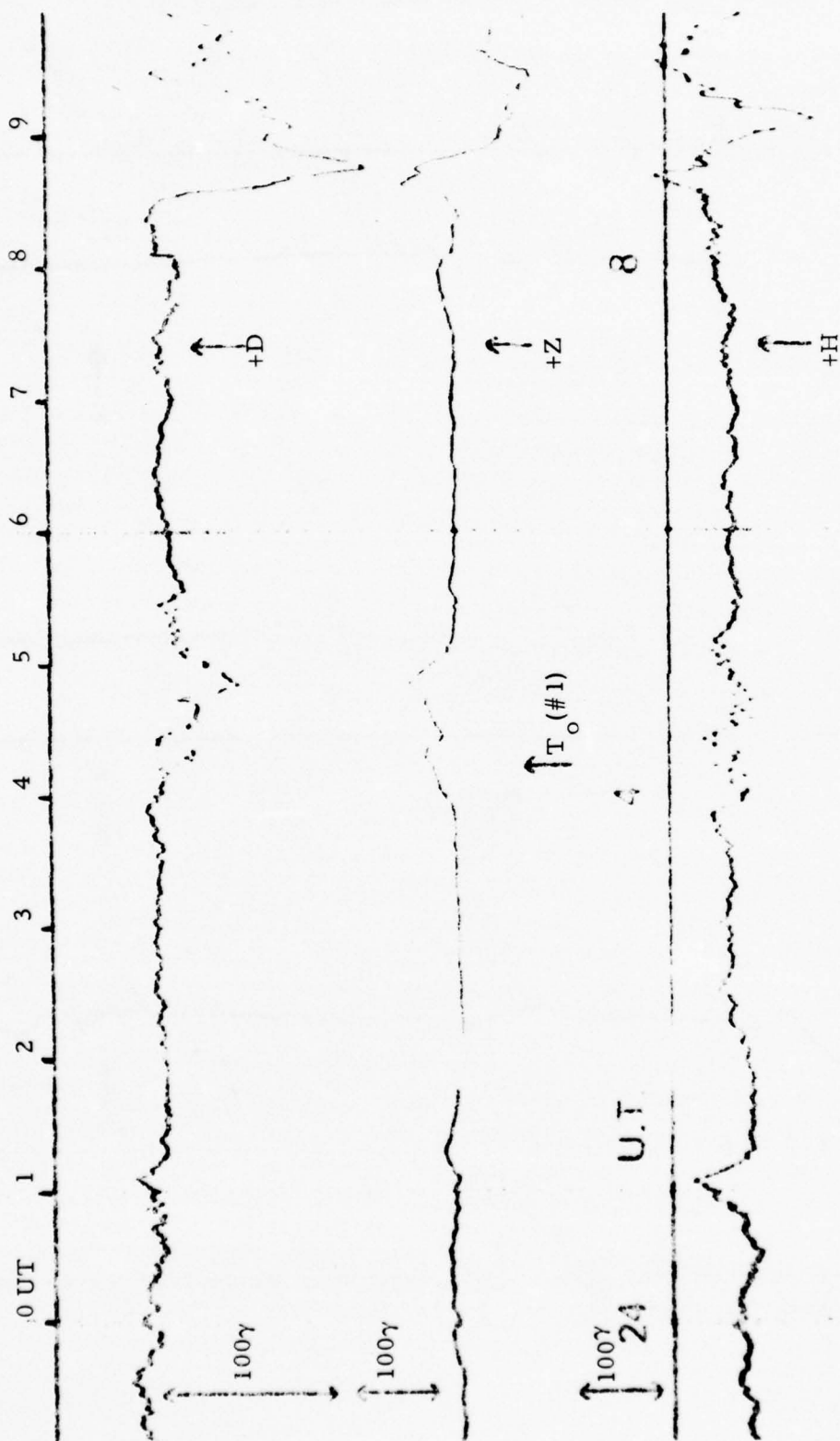


Fig. 2.16 Portion of the College Magnetometer Record for the 25 April 1975 Launches.

BEST AVAILABLE COPY

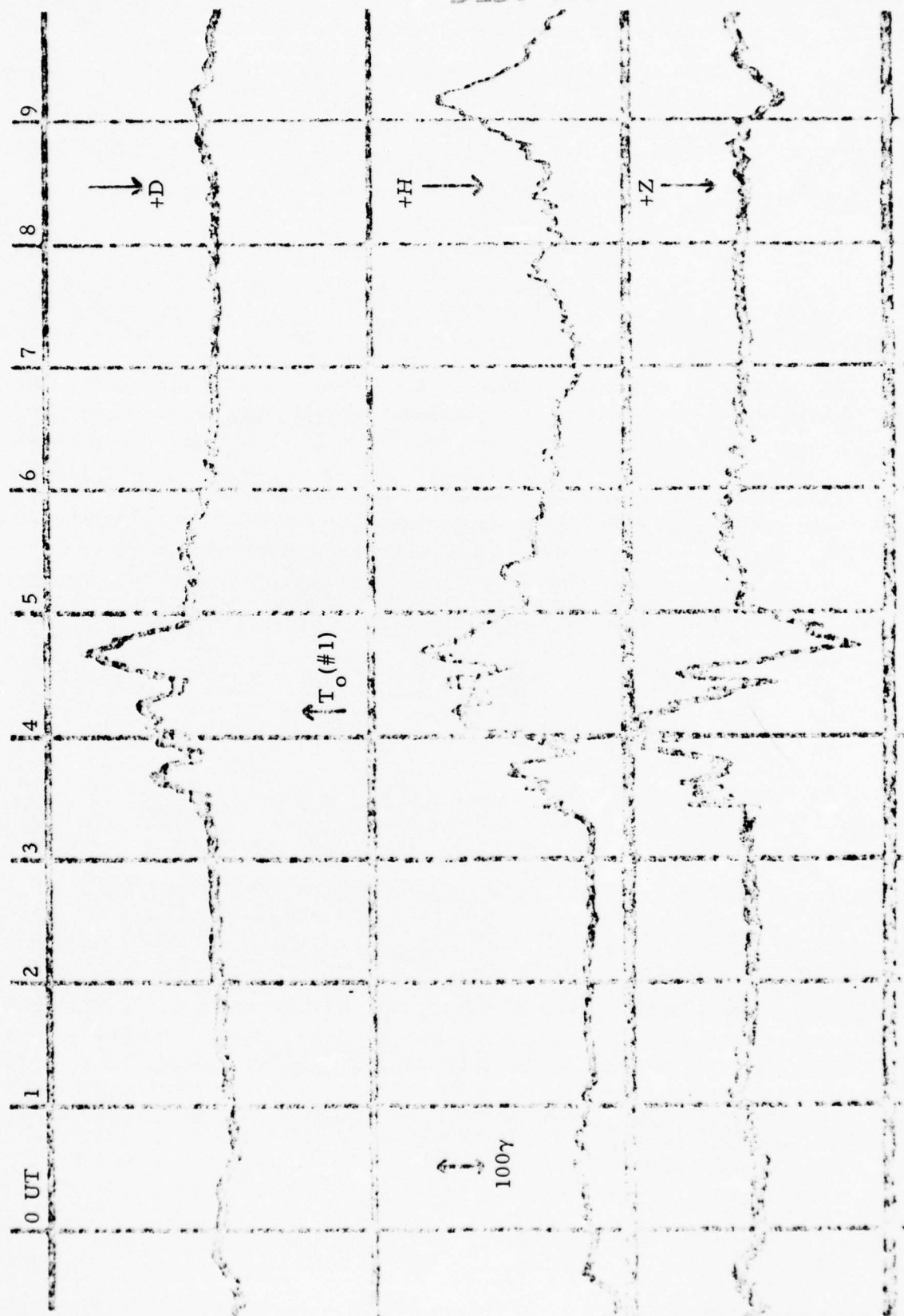


Fig. 2.17 Portion of the Great Whale River Magnetometer Record for the 25 April 1975 Launches.

BEST AVAILABLE COPY

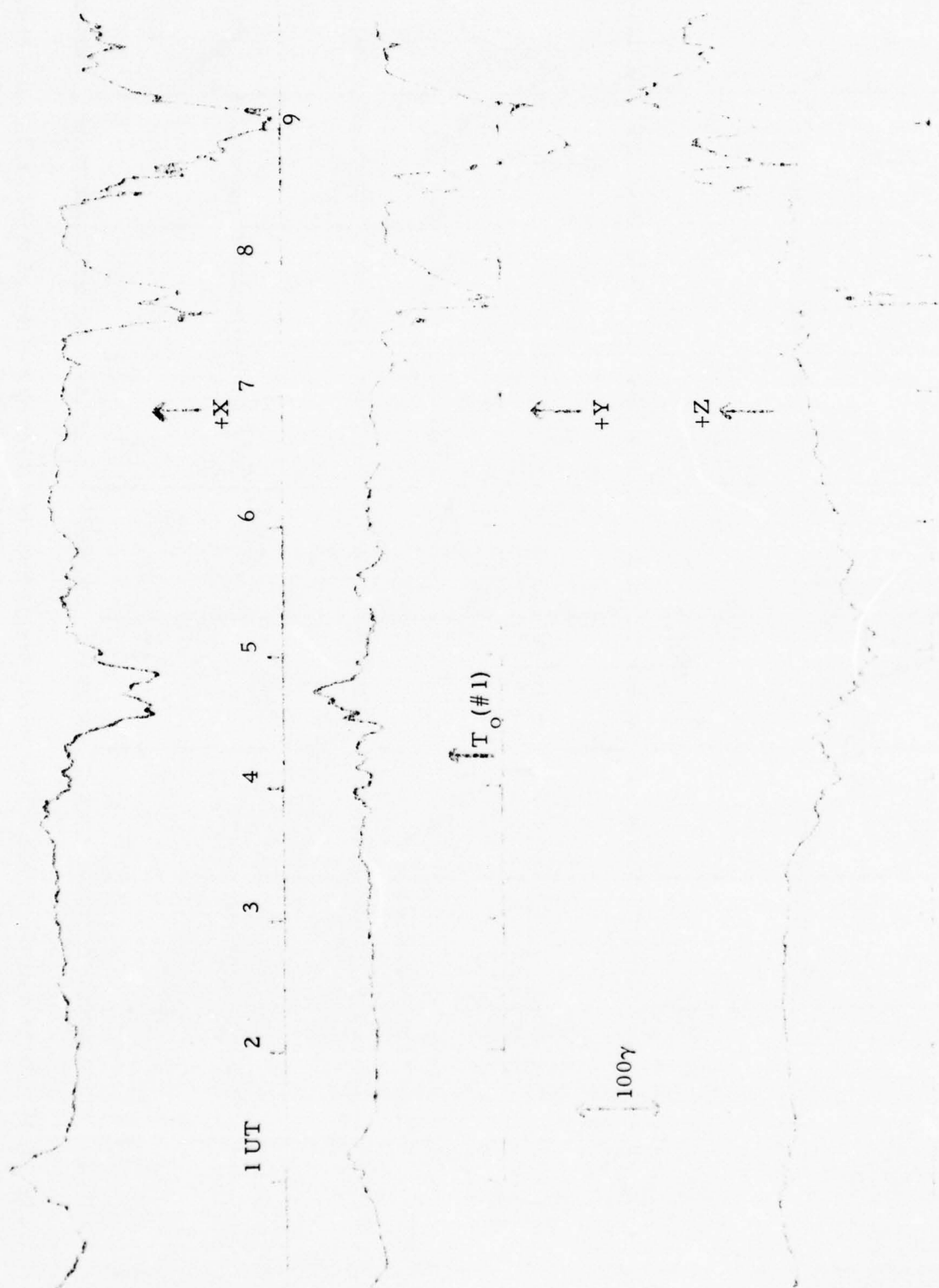


Fig. 2.18 Portion of the Yellowknife Magnetometer Record for the 25 April 1975 Launches.

BEST AVAILABLE COPY



Fig. 2.19 Portion of Ft. Smith Magnetometer Record for the 25 April 1975 Launches.

was sufficiently accurate (Refs. 1.1, 1.2 and 1.3). The real-time calculations made during the AEOLUS program used this flat earth model. Since the electrojet was generally not too far from Ft. Churchill (and O'Day) for the active launches, the usefulness of the calculations was not significantly affected.

The use of magnetometer data from many widely separated stations requires care in interpretation of results from use of a flat earth electrojet model. This is particularly true for stations far to the north or south of a westward flowing electrojet. For such stations most of the disturbance is in the vertical component, and a flat earth model would give very large (possibly infinite) distances for the electrojet. Some of the data have thus been analyzed using a cylindrical earth model, which eliminates the worst problem of the flat earth model.

The flat earth and cylindrical earth models are discussed in more detail in the following Sections. Also discussed are some of the more advanced electrojet models using field aligned currents, and induced earth current considerations. The latter models are somewhat more complete than the infinite, straight line current models, and thus more difficult to use in a real-time system, but may be useful in more extended post-flight analyses.

3.1 Flat Earth Model

The flat earth model was originally developed for the real-time electrojet instrument because of its comparative simplicity. This simplicity is essential if magnetometer data from a number of stations are to be used with a cycle period of less than one minute on a relatively simple, easily transportable, mini-computer based system. The basic geometry of the electrojet is shown in Fig. 3.1. With an infinite line current the field magnitude B can be calculated readily as

$$B = \frac{\mu_o I}{2\pi r} \quad (3.1)$$

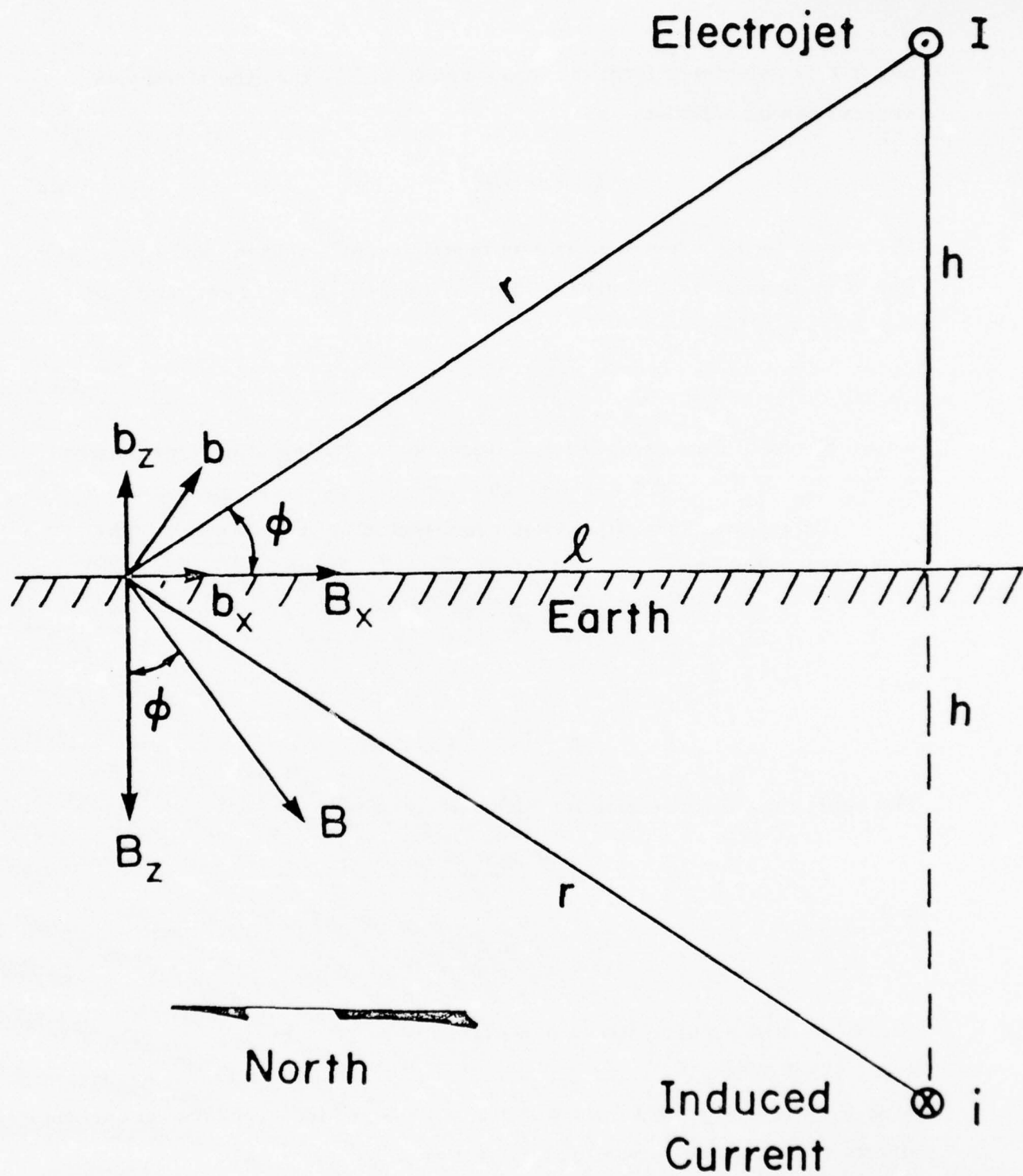


Fig. 3.1 Cross Section of Single Magnetometer Station Relative to the Auroral Electrojet.

or, if B is calculated from the measured field B_o , then the electrojet current can be calculated as

$$I = 2\pi r B / \mu_o \quad (3.2)$$

Here $\mu_o = 4\pi \times 10^{-7}$ henry/m if B is in webers/m², r in m, and I in amps. For B in gammas ($=10^{-5}$ gauss $= 10^{-9}$ webers/m²), r in km, and I in megamps this becomes

$$I = KBr \quad (3.3)$$

where $K = 5 \times 10^{-6}$ megamps \cdot km⁻¹ \cdot gamma⁻¹. The relationships between B , B_x , B_z , h , ℓ , r and ϕ are straightforward, and are given in Ref. 1.1.

Induced current effects are represented by i at depth h . The measured fields are

$$B_{ox} = B_x + b_x \quad (3.4)$$

and

$$B_{oz} = B_z - b_z \quad (3.5)$$

The approximate correction for induced currents

$$B_x = C_h B_{ox} \quad (3.6)$$

and

$$B_z = C_z B_{oz} \quad (3.7)$$

was found (Ref. 3.1) for stations in Alaska to be $C_h = 2/3$, $C_z = 3$ (see also Ref. 3.2). For the Ft. Churchill area it was found (Ref. 1.1) that a better fit is $C_h = 3/4$, $C_z = 3/2$, which gives $i = I/3$ in Fig. 3.1. Induced current effects are discussed more fully in Section 3.4.

The flat earth model first uses the measured X and Y magnetometer components to derive a direction for the electrojet flow. The horizontal

$((X^2 + Y^2)^{1/2})$ and vertical (Z) components are then corrected for induction effects by (3.6) and (3.7). The corrected disturbance fields are then used to calculate l and I in Fig. 3.1, assuming a fixed value (usually 120 km) for h .

When two or more stations are used the data generally can not be fit exactly by a single line current and an rms fit is made. The precise procedure is given in Ref. 1.1. In general, the stations must not be too far apart, in order to avoid problems with earth curvature. This generally means they must lie within a circle of less than 1000 km diameter, and the electrojet should pass through this region. For an electrojet at 120 km, it will lie on the horizon of a station on a spherical earth ($R_e = 6370$ km) when $r \simeq 1250$ km. Under these conditions $B_x \simeq 0$ in Fig. 3.1, and the flat earth model would give $r \simeq \infty$. The flat earth model is thus seen to have severe problems for stations at a large distance (more than several hundred km) from the electrojet.

3.2 Cylindrical Earth Model

The flat earth model in Fig. 3.1 can be readily modified for a cylindrical earth as shown in Fig. 3.2. For simplification, the induced earth current is not shown. Here we use only the corrected horizontal (B_h) and vertical (B_z) components, with the values being corrected by (3.6) and (3.7). From Fig. 3.2 it is seen that (R_e is the earth radius $\simeq 6370$ km)

$$\phi = \tan^{-1}(B_h/B_z) \quad (3.8)$$

$$l = R_e \alpha \quad (3.9)$$

$$r = (R_e + h) \sin \alpha / \cos \phi \quad (3.10)$$

and

$$I = KBr \quad (3.11)$$

where $B = (B_h^2 + B_z^2)^{1/2}$ and K is given after (3.3). If we set $a = R_e / (R_e + h)$, then

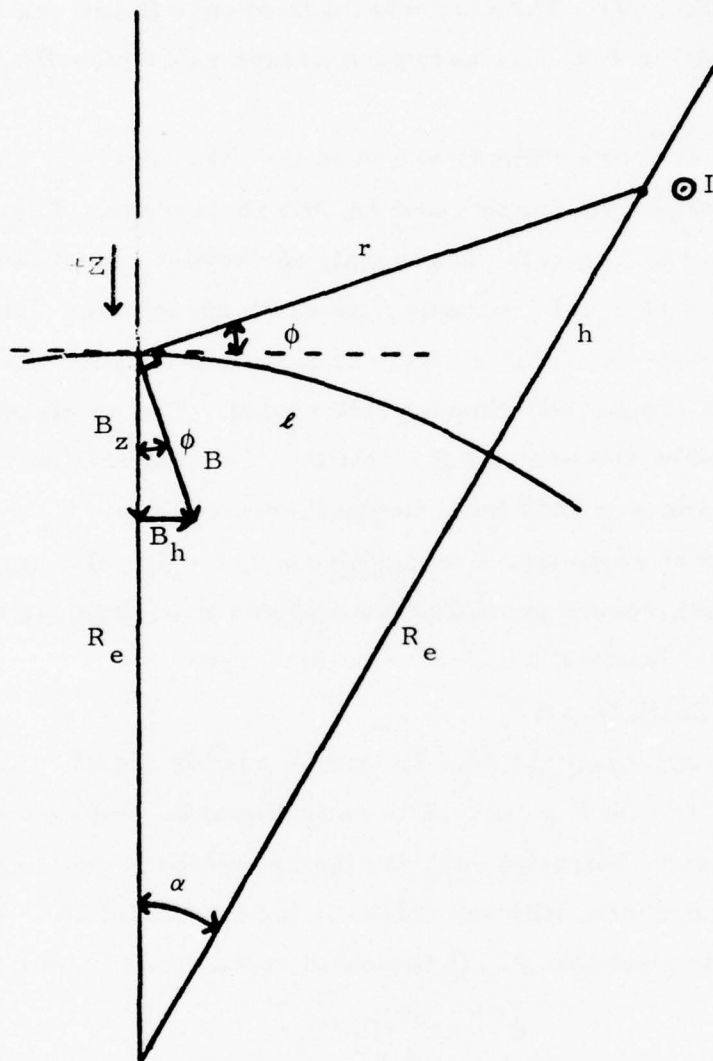


Fig. 3.2 Geometry of the Electrojet Relative to a Single Magnetometer Station in a Cylindrical Earth Model.

$$\sin \alpha = \frac{\pm \sqrt{1 - a^2 + \tan^2 \phi} - a \tan \phi}{1 + \tan^2 \phi} \quad (3.12)$$

From (3.8) to (3.12) the corrected values B_h and B_z allow the calculation of ℓ , r and I . The negative sign in (3.12) is used for a current which lies below the horizon. In Fig. 3.2, if r is extended through the (cylindrical) earth it will come to a second point at altitude h , where a current I' , flowing in the opposite direction of I , could equally well exist. The data alone cannot distinguish between I and I' , but this must be done on the basis of consistency with other stations.

The cylindrical earth model eliminates the difficulty of infinite distances in the flat earth model. However, at large (more than several hundred km) distances the infinite straight line current assumption of the model becomes increasingly bad, since the Auroral Electrojet is finite and even has non-ionospheric portions to the current path. The cylindrical earth model is nevertheless an improvement which avoids excessive complexity or long calculation times. It is best applied to single station data (assuming $h \simeq 120$ km or so), since the use of multiple stations requires greater complexity, especially if the curvature of the electrojet itself becomes significant over the array of stations used. Results using this single station approach are given in Section 4.

3.3 More General Electrojet Models

The actual configuration of the Auroral Electrojet is more a segment of current along a portion of the Auroral Zone, with field-aligned currents at each end, and closure near the equatorial plane. Calculations for currents of this configuration have been made by Kisabeth (Ref. 3.3), where results are presented for various current configurations. The models used in Ref. 3.3 are based on earlier models by Birkeland, Boström, and others, and Ref. 3.3 should be consulted for references to this earlier work. The models have been used in more recent calculations

(Ref. 3.4), and mechanisms for driving the current system have been investigated (Ref. 3.5).

The results presented in Refs. 3.3 and 3.4 show that the Auroral Electrojet can be quite complex. Westward flowing electrojets are generally a few to several degrees (latitude) in width, and a few tens of degrees in longitudinal extent. Eastward electrojets tend to predominate in the evening sector (Refs. 3.3 and 3.6), and may coexist with westward electrojets. North-south electrojet segments also seem to exist in folded auroral structures, such as westward traveling surges and north-south aligned arc segments.

The unfolding of the electrojet structure from ground station magnetometer data is a complex process. Data from many stations are required, and substantial computational capability would be required if a real-time analysis were to be attempted. Much of the data used in Refs. 3.3, 3.4 and 3.6 have come from a line of magnetometer stations in Canada, and all the analysis has been done after the fact. The complexity and cost of doing real-time electrojet analysis using these more realistic models may not be feasible at this time.

The electrojet models presented here have not been used in the analysis of the AEOLUS program magnetic activity data. The field-aligned current models have been used only as a guide in interpreting some of the data. At this time it is felt that more effort using these models on this program is not warranted.

3.4 Induced Earth Current Considerations

The measured ground station disturbance magnetic fields are composed of the direct field due to the electrojet, and the field from induced currents in the conducting portion of the earth. One of the earliest methods used for correcting the measured disturbance fields for induced current effects was to multiply the measured horizontal disturbance by $2/3$ and the vertical disturbance by 3 (Refs. 3.1 and 3.2). These values

were found to give reasonable results for the electrojet location when used for Alaskan magnetometer stations. For two nearby (≈ 100 km N-S separation) stations at Ft. Churchill it was found that better factors are $C_h = 3/4$ and $C_z = 3/2$ (Ref. 1.1)(see discussion for eqs. (3.6) and (3.7)).

The actual correction factors C_h and C_z depend on the location of the electrojet relative to the magnetometer station, as well as on local earth conductivity profiles. Because of the complexity of making a more exact correction, the simple factor method of (3.6) and (3.7) has been used frequently in the past, and is the most easily used with a real-time electrojet instrument.

A better induced current correction can be made by using a conducting earth model which assumes a perfect conductor (superconductor) beginning at some depth H_0 below the earth's surface. This method allows the induced currents to be calculated more readily. A detailed discussion in Ref. 3.3 suggests that $H_0 \approx 250$ km for this superconducting layer, and most of the electrojet analyses were made using this depth to calculate the induced current effects. For a spherical earth the superconducting shell can be exactly accounted for, with any external current configuration, by a method presented in Ref. 3.7. This method requires numerical integration, and was used in Ref. 3.3 with the field-aligned current models.

The induced currents can be readily calculated for certain simple cases. The infinite cylindrical earth model discussed earlier can have the field readily calculated from currents induced in a smaller superconducting cylinder, using the method of image currents. The appropriate geometry is shown in Fig. 3.3. In the method of image currents, $i = I$, and the superconducting boundary conditions require $B_{0z} = 0$ (no normal field) at the superconducting boundary. This can be used to obtain

$$h' = R_e - (R_e - H_0)^2 / (R_e + h) \quad (3.13)$$

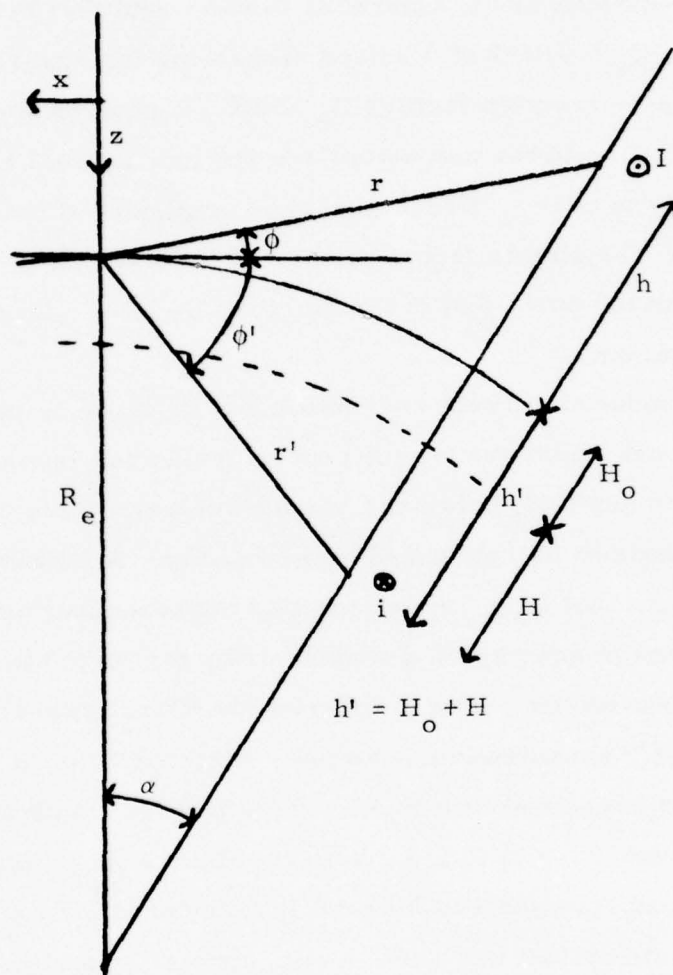


Fig. 3.3 Geometry for the Induced Currents in a Cylindrical Earth with a Superconducting Shell at Depth H_0 .

The magnetic field components can be written as

$$B_{ox} = B_x + b_x \quad (3.14)$$

where

$$B_x = - \frac{\mu_o I}{2\pi(R_e + h)} \left[\cos \alpha - \frac{R_e}{R_e + h} \right] / D \quad (3.15)$$

$$b_x = - \frac{\mu_o i (R_e + h)}{2\pi(R_e - H_o)^2} \left[\frac{R_e (R_e + h)}{(R_e - H_o)^2} - \cos \alpha \right] / D \quad (3.16)$$

$$D = \sin^2 \alpha + \left[\frac{R_e}{R_e + h} - \cos \alpha \right]^2 \quad (3.17)$$

and

$$B_{oz} = B_z - b_z \quad (3.18)$$

where

$$B_z = \frac{\mu_o I \sin \alpha}{2\pi(R_e + h)D} \quad (3.19)$$

$$b_z = \frac{\mu_o i (R_e + h) \sin \alpha}{2\pi(R_e - H_o)^2 D} \quad (3.20)$$

For the present case $i = I$, although the above equations have been given in the more general form.

The above results can be used to derive C_h and C_z as functions of for this particular model, with

$$C_h = B_x / (B_x + b_x) \quad (3.21)$$

and

$$C_z = B_z / (B_z - b_z) \quad (3.22)$$

Using $h = 120$ km, $H_0 = 250$ km, and $R_e = 6370$ km, the results (3.21) and (3.22) are plotted in Fig. 3.4. The top axis gives $l = R_e \alpha$ (α in radius), the horizontal distance to the sub-current position as measured along the (cylindrical) earth's surface (see Fig. 3.2). From Fig. 3.4 it can be seen that beyond 1000 km ($\alpha \simeq 10^\circ$) the corrections become quite large, and for C_h , even change sign. At these distances the cylindrical earth model is no longer realistic, since the ionospheric portion of the electrojet is typically only a couple thousand km long, and thus the field-aligned currents become very important.

Near the electrojet the cylindrical earth model is a rather good approximation. Table 3.1 compares values of induced (b_x) to external (B_x) field ratios calculated directly under the electrojet for the cylindrical earth model, and the more exact results of Ref. 3.3 using a field-aligned current model. Results are shown for the superconducting layer at depths of 100, 200 and 300 km. The two models give identical results at 200 km, and agree to about $\pm 20\%$ between 100 and 300 km.

Table 3.1

Comparison of Induced Current Effects in the Cylindrical Earth Model and the Field-Aligned Current Model

Depth of superconducting shell (km)	b_x/B_x ratio		Ratio ($\frac{\text{Cylindrical}}{\text{Field-Aligned}}$)
	Cylindrical Earth	Field-Aligned Currents*	
100	0.383	0.452	0.85
200	0.238	0.238	1.00
300	0.174	0.142	1.23

*From Ref. 3.3, Table 2.1, p. 53.

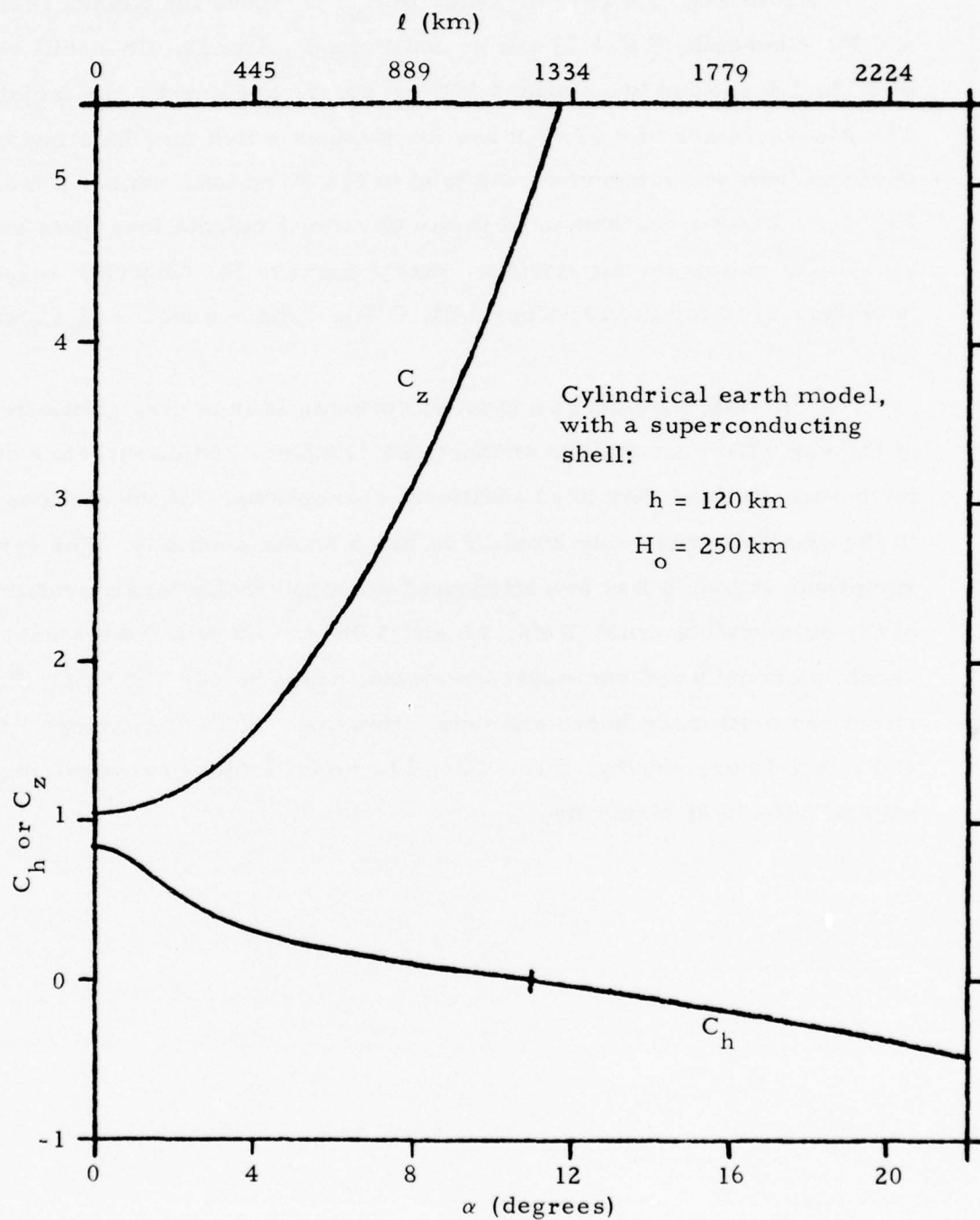


Fig. 3.4 Variation of C_h and C_z in a Cylindrical Earth Model with a Superconducting Shell.

From Fig. 3.4 the difference in C_h , C_z found for Alaska (Ref. 3.1) and Ft. Churchill (Ref. 1.1) can be understood. The Ft. Churchill values of 0.75, 1.5 are for two stations 100 km apart, and nearby electrojets. The Alaska values of 0.67, 3.0 are for stations which may be a few hundred km from the electrojet, and tend in the directions expected from Fig. 3. The corrections used in the electrojet calculations have been the Alaska values for all stations, except that the Ft. Churchill values have been used for the Ft. Churchill, O'Day (where used), and Thompson data.

One final comment on induced currents is in order. Some regions of the earth have anomalous conductivity profiles, and disturbance data from such stations may need additional corrections. Of the stations used in the present study, only Mould Bay has a known anomaly. The vertical variations at Mould Bay are attenuated by an unusually large conductivity of the surrounding crust (Refs. 3.8 and 3.9), and so data from Mould Bay should be considered somewhat uncertain, since no correction for this effect has been made in the analysis. However, since Cambridge Bay and Resolute are nearby, there should be no difficulty in recognizing any unusual effects at Mould Bay.

4. ELECTROJET CALCULATIONS FOR THE AEOLUS LAUNCHES

Two types of electrojet calculations have been done for the AEOLUS launches. The real-time calculations using the Ft. Churchill and O'Day (when available) magnetometer data, and individual station calculations made from data obtained later (Table 2.3). The real-time calculations have in some cases been redone using corrected baseline values. All real-time type calculations use the flat earth model, and Eqs. (3.6) and (3.7) to correct for induced currents ($C_h = 0.75$, $C_z = 1.5$). The individual station calculations use the cylindrical earth model, and correct for induced currents with (3.6) and (3.7). Ft. Churchill, O'Day, and Thompson had $C_h = 0.75$, $C_z = 1.5$, while all other stations had $C_h = 0.67$, $C_z = 3.0$.

The magnetically active launch set of 10 April 1975 is that most likely to yield evidence of high altitude wave phenomena. Thus most effort has been put into electrojet analysis of this event. For the magnetically quiet launches of 21 April, little electrojet analysis is possible, other than placing some limits to current intensities. The auroral launches of 25 April were not as well suited for wave phenomena detection, and were thus not as extensively analyzed as the 10 April event.

4.1 Magnetically Active Launches - 10 April 1975

The night of 10 April 1975 was quite active magnetically at Ft. Churchill. From Fig. 2.2 it can be seen that one substorm started shortly before 0700 UT, and the magnetometers were just recovering their baseline values when another substorm began somewhat after 0900 UT. This substorm began to the west of Ft. Churchill somewhat earlier, and moderate activity did not start at Ft. Churchill until about 0925 UT.

Magnetometer data from O'Day were available until just before launch of the first rocket at 0954 UT. Thus two station electrojet calculations were made from about 0925 UT to 0954 UT. The electrojet calculations for Ft. Churchill and O'Day (where available) are shown in Fig. 4.1. The two station data agree reasonably well, and indicate that the electrojet

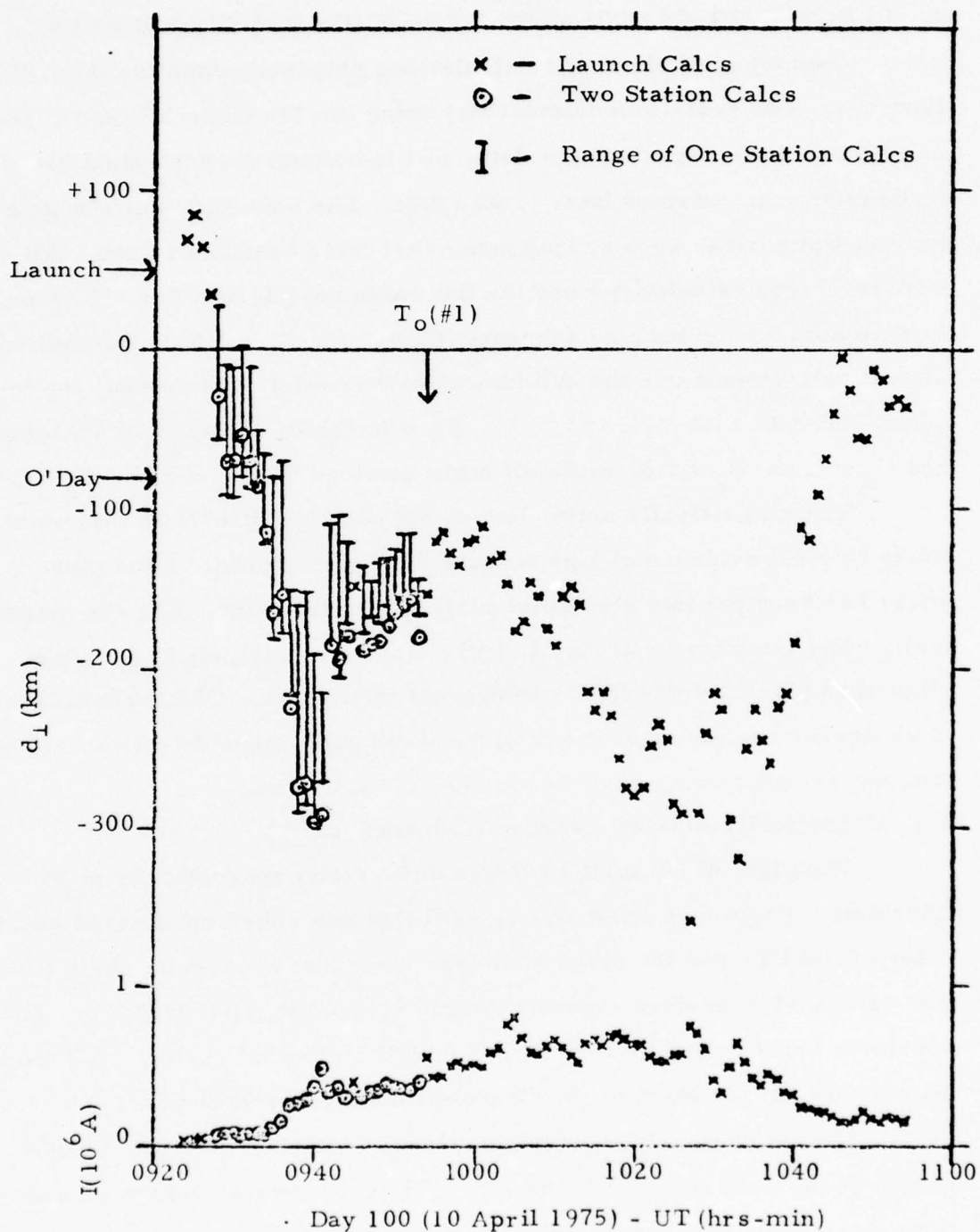


Fig. 4.1 Electrojet Parameters Calculated from the Ft. Churchill and O'Day Magnetometer Data for the Active Launches of 10 April 1975.

might be some tens of km wide. The strong motion and intensification centered about 0940 UT appear promising for the generation of upper atmosphere waves.

The activity at Ft. Churchill can be roughly divided into three periods. The first is 0925-0940 UT, and consists primarily of a negative step in the X component, with the Y and Z components showing much less activity. The second period is roughly 0945-1000 UT, and consists of a larger negative step in X, a negative step in Y, and a positive step in Z. This period shows significant substructure, particularly in the X component. The third period from 1005-1020 UT is to a large extent a decay period, with X going less negative, Y holding steady, and Z holding steady at a moderately strong positive value. Thereafter the activity continues to decay before another disturbance begins at about 1040 UT.

The rough three period structure shows up at most other stations listed in Table 2.2, and this has been used as the basis for constructing electrojet maps for each period. These maps are given in Figs. 4.2, 4.3 and 4.4, and were calculated for the average disturbance during each period, using the cylindrical earth model. In Fig. 4.1, for the 0925-0940 UT period, the electrojet is clearly centered to the west of Ft. Churchill, with the most intense portion being between College and Meanook. Electrojet intensity appears to be about 10^6 A. Ft. Churchill may not yet be under the electrojet at this time, but is at the eastern end of a westward electrojet with some influence from the field-aligned current at this end.

The second period, shown in Fig. 4.3, shows the electrojet having shifted to the Ft. Smith-Ft. Churchill area, with activity at College and Sitka being comparatively weak. The calculated currents for these latter two stations are shown in parentheses, since they are based on small disturbances and can be changed significantly by small adjustments to the baseline values. The baseline values for all stations were taken to be

BEST AVAILABLE COPY



Fig. 4.2 Single Station Electrojet Map for 0925-0940 UT on 10 April 1975.

BEST AVAILABLE COPY



Fig. 4.3 Single Station Electrojet Map for 0945-1000 UT on 10 April 1975.

BEST AVAILABLE COPY



Fig. 4.4 Single Station Electrojet Map for 1005-1020 UT on 10 April 1975.

the values existing shortly after 0900 UT, just before the disturbance began.

The third period is shown in Fig. 4.4, and here the electrojet has expanded, going from Ft. Churchill to at least College. Some weakening in the center, near Ft. Smith and Yellowknife, is evident, with the electrojet being well north of Meanook at this time.

A few general observations are in order. The data from Baker Lake are taken from a very poor record, and so are questionable. They appear to fit with the Ft. Churchill, Thompson and Cambridge Bay calculations, and so have been included in the electrojet maps. The magnetometer data from Narssarssuaq and Leirvogur are weak and irregular, being far to the east of the electrojet, and so no calculations have been made for these two stations. Finally, the calculations for Mould Bay appear to be in reasonable agreement with the Resolute and Cambridge Bay results, so the effect of conductivity anomaly (Refs. 3.8 and 3.9) is not very evident in this event.

The current intensity calculated from the disturbance at each station is shown by the length of the arrow, with the scale being given in Fig. 4.2. There is a general trend for the current to increase with distance from the station. This is most noticeable in the Yellowknife, Ft. Smith, and Sitka calculations in Fig. 4.2, when they are compared to the Meanook results. This effect would be even larger if the C_h , C_z vs. distance curves in Fig. 3.4 were used, since this would increase the corrected disturbance at large distances where the disturbance is mostly in the Z component.

The above effect is most likely due to the field-aligned currents at the eastern and western ends of the electrojet. Directly under the center of the electrojet the disturbance is mostly horizontal, with the two field-aligned components adding together, and both reducing the disturbance from the ionospheric current segment. From calculations in Ref. 3.3 (Fig. 2.4, p. 30), the field-aligned currents contribute about +300 γ to H

while the ionospheric current gives -800γ , and these add to the total measured disturbance of -500γ . About 10° north of the electrojet the contributions to Z are -10γ , $+70\gamma$, and a total Z disturbance of $+60\gamma$. Moving north (or south) of the electrojet causes the disturbances from the field-aligned currents to cancel and so increases the fraction of the net observed disturbance due to the ionospheric current leading to the effect mentioned above. A rough correction for this effect could be made, but in view of other neglected factors it is not likely to make much of an improvement in the usefulness of Figs. 4.2, 4.3 and 4.4. The major usefulness of these electrojet maps is in giving a general view of the electrojet configuration, and some error in intensity, location, and direction will not significantly affect this purpose.

The structure of the disturbance at Meanook (Fig. 2.5) suggests that, at least before 1000 UT, the electrojet was centered over Meanook (Figs. 4.2 and 4.3), and consisted of several pulsations or "arcs". The times and disturbance ranges at Meanook for nine of these arcs are given in Table 4.1. All disturbance values are referenced to the 0900 baseline values, so successive arc disturbance values may be somewhat influenced by the preceding arc. The disturbance values are thus the total disturbance during each arc period, and only partially that due to each individual arc. Note that the word "arc" as used here refers to the pulsations observed in the H component, and may or may not be correlated with actual auroral arcs.

The electrojet parameters for the Meanook arcs are given in Table 4.2. These are calculated from the disturbance values in Table 4.1 using the cylindrical earth model and C_h , $C_z = 0.67$, 3.0 . The results show that the electrojet started about 200 km south of Meanook, and ended about 200 km north of Meanook. The electrojets generally flowed at an angle of -60° to north, i. e., 30° north of due west. Variations were generally about $\pm 10^\circ$, with the extreme being $\pm 15^\circ$.

Table 4.1

Magnetic Disturbance Values for Several "Arcs"
at Meanook for the 10 April 1975 Event

Time of arc (average)* (UT-hrs min)	Time width of arc (min)	Time interval between arcs (min)	H disturb- ance (γ)	D disturb- ance** (γ)	Z disturb- ance** (γ)
0912.2	2.7	}	-165	-15	+60, +80
(0920.3)	5.4		-285	(-55)	+55, +25
0926.2	5.4	}	-465	-85	+70, +10
0931.1	2.7		-585	-15, -65	+25, +50
0935.7	4.1	}	-610	-10, -100	+15, +80
0942.7	2.7		-490	+5, -140	-25, +40
0948.1	3.2	}	-410	-165, -65	-15, -50, +15
0955.4	3.2		-185	-50, -5	+25, -35
1000.5	5.4	}	-155	0, +15	-40, -90

*0920.3 arc may be two, at 0918.9 and 0920.5.

**D value in parentheses may be composed of two subarcs. Two or more values give the range over the duration of the arc time.

Table 4. 2

Electrojet Parameters for the Meanook "Arcs"
for the 10 April 1975 Event

Time of arc (average)* (UT-hrs min)	ℓ/I : ℓ is perpendicular distance to sub-arc position (km). I is current intensity in 10^6 A.**		
	<u>start</u>	<u>middle</u>	<u>end</u>
0912. 2	-191/0. 24		-250/0. 36
(0920. 3)	-102/0. 20		-46/0. 13
0926. 2	-80/0. 27		-11/0. 19
0931. 1	-23/0. 24		-46/0. 27
0935. 7	-13/0. 25		-70/0. 33
0942. 7	+28/0. 21		-42/0. 23
0948. 1	+18/0. 18	+60/0. 22	-20/0. 17
0955. 4	-70/0. 10		+101/0. 13
1000. 5	+138/0. 14		+295/0. 46

*0920. 3 arc may be two, at 0918. 9 and 0920. 5.

**Currents are generally flowing at an angle of -60° ($\pm 10^\circ$), towards west-north-west. Negative ℓ is south of Meanook.

Arc structure is also observable to some degree at most other stations. The Ft. Churchill and Thompson data show several such arcs which can be correlated with the Meanook arcs. A comparison of the principal arc times at Meanook, Ft. Churchill, and Thompson is given in Table 4.3.

From Figs. 4.2 and 4.3 it is seen that prior to 0945 UT the activity was all west of Ft. Churchill, apparently terminating just to the east of Meanook. This suggests that most of the Meanook arcs were electrojets terminating in a field-aligned current near Meanook. Using this assumption and further assuming that each arc at Meanook generates a high altitude "wave", the arrival times of these waves at the Ft. Churchill area can be calculated for any assumed wave velocity. Using a wave velocity of 700 m/sec then gives the "wave" arrival times at Ft. Churchill listed in Table 4.4. The varying times to reach Ft. Churchill are because the north-south shift of the electrojet relative to Meanook, as given by the average ℓ values from Table 4.2, were used to correct the distance the "wave" has to travel to reach Ft. Churchill.

The final column in Table 4.4 gives the time interval between wave crests at Ft. Churchill. A five minute period predominates, as it does in the Meanook arcs alone as shown in Table 4.1. For times after 1000 UT the Ft. Churchill area may have a more complex wave pattern than suggested by Table 4.4 alone. The strong electrojet activity near Ft. Churchill after 0945 UT may lead to wave phenomena at Ft. Churchill due primarily to nearby generation. However, the arc times for Ft. Churchill and Thompson in Table 4.3 suggest that a strong five minute periodicity is the most likely to be present. Whether such high altitude waves were in fact generated, and more importantly, whether they can be observed in the AEOLUS chemical release experiments, can not be answered by the magnetometer data or electrojet calculations. The results presented here can only suggest possible effects to look for in the analysis of the chemical release data.

Table 4. 3

Comparison of "Arc" Times at Meanook, Ft. Churchill,
and Thompson, for the 10 April 1975 Event

Times in UT hrs-min for arcs at:

<u>Meanook</u>	<u>Ft. Churchill *</u>	<u>Thompson*</u>
0912. 2		
0920. 3		
0926. 2	0926. 5	0926. 4
0931. 1	0930. 3	0932. 3
0935. 7	0935. 1	0934. 4
		0937. 8
0942. 7	0941. 4	0942. 8
0948. 1	0949. 2	0947. 0
0955. 4	0955. 4	0955. 8
1000. 5	(1000. 0)	(1000. 0)
	1002. 7	1004. 1
	1010. 8	1010. 2
	1015. 4	1015. 5
	1022. 4	1022. 4
	1028. 1	1029. 0
		1033. 5

*The arcs at 1000. 0 at Ft. Churchill and Thompson are
weak and thus questionable.

Table 4. 4

Calculated Arrival Times of Meanook "Waves" at Ft. Churchill
for the April 10 1975 Event

Meanook arc time* (UT-hrs min)	Time to reach Ft. Churchill (min)**	Ft. Churchill wave peak time (UT-hrs min)	Time interval between waves (min)
0912. 2	35. 0	0947. 2	{ 5. 1
(0920. 3)	32. 0	0952. 3	
0926. 2	31. 4	0957. 6	{ 4. 7
0931. 1	31. 2	1002. 3	
0935. 7	31. 3	1007. 0	{ 6. 3
0942. 7	30. 6	1013. 3	
0948. 1	30. 5	1018. 6	{ 7. 0
0955. 4	30. 2	1025. 6	
1000. 5	26. 0	1026. 5	{ 0. 9

*0920. 3 arc may be two, at 0918. 9 and 0920. 5.

** See text for explanation of calculation method.

The electrojet calculations suggest that the possibility of observing high altitude waves in the magnetically active launches of 10 April 1975 is excellent. Pulsation activity is strongly present at times that can readily lead to waves in the Ft. Churchill area during the optimum observation time. Since $T_0 = 0954$ UT for the first rocket, the optimum observation time begins shortly before 1000 Ut, and lasts perhaps 10 to 15 minutes. The magnetically active launch thus appears to have had excellent magnetic activity when referred to the AEOLUS program objectives.

4.2 Magnetically Quiet Launches - 21 April 1975

Little electrojet analysis can be performed for the magnetically quiet launches of 21 April 1975, since there was no noticeable electrojet present. From the Ft. Churchill record in Fig. 2.10, the most noticeable activity within an hour of launch was an approximately -20% jump in X at about 0845 UT. This corresponds to an overhead westward electrojet of about 0.01 MA intensity, a very weak electrojet which is within the noise level typically observed with the electrojet instrument. This step at 0845 in the Ft. Churchill record shows up as a small oscillation at most other stations (see, e. g., Figs. 2.12 and 2.13).

The launches of 21 April thus took place with no significant electrojet activity present during, or for some hours before, the rocket launches. Possible electrojet intensities are less than a few times 0.01 MA, through the auroral zone from College to Leirvogur. This set of launches is thus an excellent one for background measurement to ensure that any motion observed in the 10 April set is real and not due to statistical fluctuations in the data.

4.3 Auroral Launches - 25 April 1975

The auroral launches of 25 April 1975 occurred about two hours before local midnight, T_0 for the first rocket being at 0413 UT. The launches were into an active aurora, accompanied by significant magnetic activity. The event was moderately complex, as can be seen in the

Ft. Churchill magnetometer record in Fig.2.14. Since the launch occurred during darkness for the upper atmosphere, the information obtained from the chemical releases is not as great, so an extensive electrojet analysis for this event has not been made.

The magnetometer data from Ft. Churchill and O'Day were analyzed for electrojet parameters, using the flat earth model of the electrojet instrument. The results are shown in Fig. 4.5, with the two station calculations being possible only for about a 15 minute period before launch. At about 0430 UT the Ft. Churchill Z component became very negative, while the X and Y components became small, indicating a large current to the north. At this time the electrojet calculations become quite uncertain because of the large distance of the electrojet from Ft. Churchill, and so the points are enclosed in parentheses. It is questionable whether the electrojet actually did make a large northward excursion, as the strong motion shown in Fig. 4.5 is quite likely the result of fitting a complex current system with too simple a model.

The electrojet activity is very pronounced, with significant excursions north and south over the Ft. Churchill area. The two station calculations are generally in excellent agreement with the single station calculations, as shown by the small spread in d_{\perp} shown in Fig. 4.5. The intensity of the electrojet current is less than that for the 10 April event (Fig.4.1).

The large amount of electrojet motion over the Ft. Churchill area is likely to make the observation of high altitude waves difficult. The superposition of waves generated at different locations can result in canceling of large motions, with short-period motion predominating. The lesser chance of observing wave motion in this event, compared with the 10 April event, has resulted in most emphasis being placed on the 10 April event. The possibility of some wave motion being present for the 25 April event is moderately strong, however, so further analysis might be desirable, should the analysis of the chemical release data show significant results.

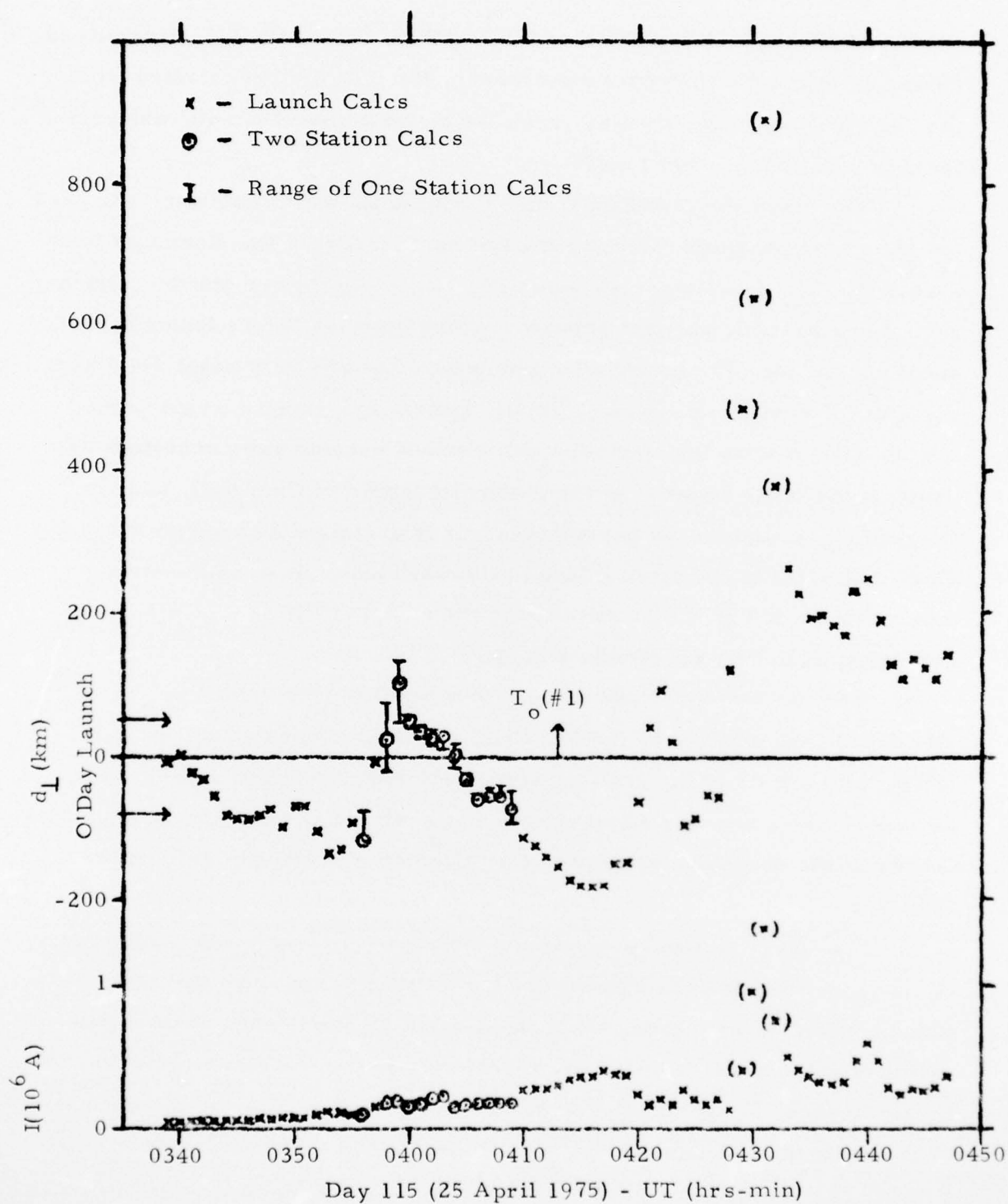


Fig. 4.5 Electrojet Parameters Calculated from the Ft. Churchill and O'Day Magnetometer Data for the Auroral Launches of 25 April 1975.

5. SUMMARY OF MAGNETIC AND ELECTROJET CONDITIONS FOR THE AEOLUS LAUNCHES

5.1 Magnetically Active Launches - 10 April 1975

The magnetically active launches of 10 April 1975 took place during a magnetic substorm that appears very promising for the generation of high altitude waves. The first rocket was launched at 0954 UT, while the substorm started shortly after 0900 UT.

The magnetic activity can be separated into three rough periods. The first, from about 0925 to 0940 UT, had the electrojet and magnetic activity occurring mainly from Meanook west to at least College. During this period Meanook was most likely near the eastern end of the westward electrojet, near the field-aligned current at this end of the ionospheric electrojet. Strong, roughly five minute pulsations at Meanook appear promising for the generation of waves which might be observable at Ft. Churchill some half hour or so later, depending on wave velocity.

The second period, from about 0945 to 1000 UT, had the main activity shift to the Ft. Smith to Ft. Churchill region. Pulsations visible at Ft. Churchill and Thompson again look promising for wave generation. The activity in X at Ft. Churchill peaks at about 1005 UT.

The third period, from about 1005 to 1020 UT, had the activity centered near Ft. Churchill as it decayed. Pulsations are still evident in the Ft. Churchill X component, but this period is too late to influence the chemical release data.

The launch activity was preceded by a smaller event from about 0700 to 0830 UT, and followed (at Ft. Churchill) by stronger activity from about 1030 to 1230 UT. The entire launch period was quite active, with $K_p = 4+$.

The Auroral Electrojet near Ft. Churchill reached a moderate intensity at about 0935 UT, and was centered about 200 km south of the launch area. Sharp motions occurred at about 0940 UT and this type activity is very promising for high altitude wave generation. The electrojet calculations

for Ft. Churchill and O'Day are in reasonable agreement, indicating that the primary activity was associated with a single electrojet. The westward electrojet current was about 0.5 MA during most of the period from about 0940 to 1040 UT.

5.2 Magnetically Quiet Launches - 21 April 1975

The magnetically quiet launches of 21 April 1975 took place during a period with $K_p = 3$, preceded by 2 and 2+. Disturbances from College to Leirvogur show less than a few tens of gammas amplitude for some five hours before the launches. The first rocket was launched at $T_o = 0907$ UT, and moderate magnetic activity began after 1030 UT, with a peaking near 1230 and 1400 UT. The earliest pre-launch activity was centered at about 0200 UT, with recovery complete by 0400 UT. These launches thus took place with magnetic conditions considerably different from the 10 April launches, and it is unlikely that electrojet-generated high altitude waves were present.

While magnetic conditions can be more quiet, the 21 April launches took place during a period of no significant Auroral Electrojet activity for more than five hours preceding, and more than one hour following, the launch of the first rocket. The electrojet current was less than a few $\times 0.01$ MA during this entire period.

5.3 Auroral Launches - 25 April 1975

The auroral launch set began with the launch of the first rocket at 0413 UT on 25 April 1975. The associated magnetic activity began at about 0330 UT, and was quite widespread, covering the Auroral Zone from at least College on the west to Leirvogur on the east. At Ft. Churchill the electrojet started to the south and moved north near 0430 UT. Much structure is present in the magnetometer traces.

The auroral launches were during a period with $K_p = 3-$, so the magnetic activity was not as intense as for the 10 April launches. This is particularly shown by the electrojet current intensity calculations for Ft. Churchill

and C'Day, which average about half of the intensity for the 10 April event. The electrojet was, however, located closer to the launch area, and showed more motion than the 10 April event. The 25 April electrojet is more nearly a single, narrow line current, as shown by the significantly better agreement of the Ft. Churchill and O'Day calculations.

6. CONCLUSIONS AND RECOMMENDATIONS

The study of the magnetic conditions for each of the three sets of rocket launches in the AEOLUS program shows that the objectives for magnetic conditions were met. Specifically:

- i) The magnetically active launch set of 10 April 1975 was during a period of significantly active magnetic conditions. K_p was 4+, the disturbance at Ft. Churchill was about -500 γ in H, and the electrojet current was about 0.5 MA. Significant electrojet movement 15 to 20 minutes before launch of the first rocket makes the existence of high altitude waves more likely. The magnetometer pulsations observed at Ft. Churchill and Meanook are also good indicators that this launch set might allow the observation of high altitude waves.
- ii) The magnetically quiet launch set of 21 April 1975 was during a period of moderate magnetic quiet for five hours before to one hour after launch of the first rocket. While the succeeding K_p values were 2+, 2 and 3, the maximum magnetometer variations observed during this period were a few tens of gammas. The electrojet intensity was generally less than a few \times 0.01 MA. This launch set thus was for magnetic conditions significantly different from the 10 April launch set, and should provide a suitable background measurement for the chemical release data.
- iii) The auroral launch set of 25 April 1975 was also accompanied by significant magnetic activity. The disturbance was less than the 10 April event, but the electrojet calculations showed more

movement of the current system. The electrojet was located between Launch (Ft. Churchill) and O'Day for most of the event. The following recommendations are made:

- i) Should high altitude waves be detected, particularly for the magnetically active launch set of 10 April, then it may be desirable to analyze the event in small time steps using the more realistic field-aligned current models. Since this is likely to be time consuming, it should be considered only after positive detection of high altitude waves.
- ii) The real-time electrojet instrument should be used in conjunction with any possible future programs for the detection of phenomena generated by, or associated with, the Auroral Electrojet. The instrument has shown that it can provide useful additional calculations which can help in making launch decisions.

REFERENCES

- 1.1 B. Sellers, F. A. Hanser, and P. Morel, Design, Fabrication and Use of an Instrument for Real-Time Determination of Polar Electrojet Position and Current Parameters, AFCRL-TR-73-0166 (March 1973).
- 1.2 B. Sellers, F. A. Hanser, and P. P. Vancour, An Instrument for Real-Time Determination of Polar Electrojet Position and Current Parameters, Rev. Sci. Inst., 44, 888 (1973).
- 1.3 F. A. Hanser, B. Sellers, and R. P. Vancour, The Real-Time Determination of Ionospheric Current Parameters during a Substorm, J. Geomagn. Geoelectr., 25, 339 (1973).
- 1.4 F. A. Hanser and B. Sellers, Analysis of Ground Station Magnetometer Data Obtained During the Rocket Launches in the AEOLUS Program, April 1975, at Ft. Churchill, Manitoba, Scientific Report submitted for approval to AFGL (October 1976).
- 3.1 S.-I. Akasofu, Large-scale Auroral Motions and Polar Magnetic Disturbances - I, A Polar Disturbance at about 1100 Hours on 23 September 1957, J. Atm. Terr. Phys., 19, 10-25 (1960).
- 3.2 S.-I. Akasofu, S. Chapman and A. B. Meinel, The Aurora, pp. 1-158 in Handbuch der Physik, Vol. XLIX/1, Geophysics III, Part 1, edited by S. Flugge, Springer-Verlag, Berlin (1966).
- 3.3 J. L. Kisabeth, The Dynamical Development of the Polar Electrojets, Ph.D Thesis, Dept. of Physics, Univ. of Alberta, Edmonton, Canada (1972).
- 3.4 J. L. Kisabeth and G. Rostoker, Current Flow in Auroral Loops and Surges Inferred from Ground-Based Magnetic Observations, J. Geophys. Res., 78, 5573-84 (1973).
- 3.5 G. Postoker and R. Boström, A Mechanism for Driving the Gross Birkeland Current Configuration in the Auroral Oval, J. Geophys. Res., 81, 235-44 (1976).
- 3.6 D. D. Wallis, C. D. Anger, and G. Postoker, The Spatial Relationship of Auroral Electrojets and Visible Aurora in the Evening Sector, J. Geophys. Res., 81, 2857-69 (1976).

- 3.7 A. A. Ashour, The Evaluation of the Field of the Currents Induced in the Earth by an External Field Whose Distribution is Known Numerically, Radio Sci., 6, 171-3 (1971).
- 3.8 P. A. Camfield and D. I. Gough, Comment on Use of Anomalous Stations for IMS, EOS, Trans. Am. Geophys. Union, 57, 850 (1976).
- 3.9 J. M. DeLaurier, L. K. Law, E. R. Niblett, and F. C. Plet, Geomagnetic Variation Anomalies in the Canadian Arctic, 2, Mould Bay Anomaly, J. Geomagn. Geoelec., 26, 223-45 (1974).

least College on t
electrojet started
ture is present in

The auror
netic activity was
ticularly shown b